Journal of Radiation Research, Vol. 64, No. 2, 2023, pp. 228–249
https://doi.org/10.1093/jrr/rrad003
Advance Access Publication: 11 February 2023

Molecular and cellular basis of the dose-rate-dependent adverse effects of radiation exposure in animal models. Part II: Hematopoietic system, lung and liver

Keiji Suzuki[1,†,*], Tatsuhiko Imaoka[2,†], Masanori Tomita[3,†], Megumi Sasatani[4,†], Kazutaka Doi[5], Satoshi Tanaka[6], Michiaki Kai[7], Yutaka Yamada[2] and Shizuko Kakinuma[2]

[1]Department of Radiation Medical Sciences, Atomic Bomb Disease Institute, Nagasaki University, 1-12-4 Sakamoto, Nagasaki 852-8523, Japan
[2]Department of Radiation Effects Research, National Institute of Radiological Sciences (NIRS), National Institutes for Quantum Science and Technology (QST), 4-9-1 Anagawa, Inage-ku, Chiba 263-8555, Japan
[3]Biology and Environmental Chemistry Division, Sustainable System Research Laboratory, Central Research Institute of Electric Power Industry (CREIPI), 2-11-1 Iwado Kita, Komae, Tokyo 201-8511, Japan
[4]Department of Experimental Oncology, Research Institute for Radiation Biology and Medicine, Hiroshima University, 1-2-3 Kasumi, Minami-ku, Hiroshima 734-8553, Japan
[5]Department of Radiation Regulatory Science Research, National Institute of Radiological Sciences (NIRS), National Institutes for Quantum Science and Technology (QST), 4-9-1 Anagawa, Inage-ku, Chiba 263-8555, Japan
[6]Department of Radiobiology, Institute for Environmental Sciences, 1-7 Ienomae, Obuchi, Rokkasho-mura, Kamikita-gun, Aomori 039-3212, Japan
[7]Nippon Bunri University, 1727-162 Ichiki, Oita, Oita 870-0397, Japan
*Corresponding author, Department of Radiation Medical Sciences, Nagasaki University Atomic Bomb Disease Institute. 1-12-4 Sakamoto, Nagasaki 852-8523, Japan. Tel:+81-95-819-7116; Fax:+81-95-819-7117; E-mail: kzsuzuki@nagasaki-u.ac.jp
[†]K. Suzuki, T. Imaoka, M. Tomita and M. Sasatani contributed equally.
(Received 16 April 2022; revised 4 October 2022; editorial decision 9 January 2023)

ABSTRACT

While epidemiological data have greatly contributed to the estimation of the dose and dose-rate effectiveness factor (DDREF) for human populations, studies using animal models have made significant contributions to provide quantitative data with mechanistic insights. The current article aims at compiling the animal studies, specific to rodents, with reference to the dose-rate effects of cancer development. This review focuses specifically on the results that explain the biological mechanisms underlying dose-rate effects and their potential involvement in radiation-induced carcinogenic processes. Since the adverse outcome pathway (AOP) concept together with the key events holds promise for improving the estimation of radiation risk at low doses and low dose-rates, the review intends to scrutinize dose-rate dependency of the key events in animal models and to consider novel key events involved in the dose-rate effects, which enables identification of important underlying mechanisms for linking animal experimental and human epidemiological studies in a unified manner.

Keywords: radiation; low dose; low dose rate; cell; animal; cancer; epidemiology

INTRODUCTION

After the Fukushima Daiichi Nuclear Power Plant accident, the health effects of exposure to low-dose and low-dose-rate radiation have attracted much attention, Although the linear non-threshold (LNT) model is currently applied to estimate cancer risk, however, the scientific evaluation of the LNT model is still insufficient. It results in the multiple layers of discomfort that hinders the resilience and recovery of the affected areas [1].

While the International Commission on Radiological Protection (ICRP) has applied the dose and dose-rate effectiveness factor (DDREF) of 2 from cancer risk estimates derived from epidemiological studies of A-bomb survivors [2–4], the value of DDREF has been debated [5, 6]. Recent animal models have made significant contributions to provide quantitative data and mechanistic insights on this issue [7–9], and they are apparently the clue to understand the dose-rate effects [10, 11]. Therefore, the current review aims at

compiling animal studies with respect to dose-rate-dependent adverse effects.

Recently, the application of the adverse outcome pathway (AOP), together with that of the 'key events' leading to the outcome, has been discussed [5]. Since little information was available in animal models [12, 13], experimental studies using animals at different dose rates are reviewed herein. We intend to scrutinize the dose-rate dependency of the novel key events (Table 1), which should enable unifying the underlying critical mechanisms to connect animal experimental studies with human epidemiological studies.

In conjunction with the accompanying review article, this review continues compiling data from animal studies of three tissues, namely hematopoietic tissue, lung and liver.

The definition of low-dose and low-dose-rate herein follows the consideration by UNSCEAR. An ionizing radiation dose of <100 mGy is considered as being low dose, and a dose rate of <0.1 mGy/min averaged over 1 h (corresponding to 6 mGy/h) is regarded as low-dose-rate [14].

STUDIES TOWARDS UNDERSTANDING THE MECHANISMS UNDERLYING DOSE-RATE EFFECTS IN ANIMAL EXPERIMENTS

Summary of *in vivo* studies towards cancer development

This section reviews dose-rate effects in animal experiments concerning hematopoietic system, lung and liver and discusses the possible underlying mechanisms with respect to AOP.

Hematopoietic system

The hematopoietic system generates and maintains both a stable number of all type of blood cells and immune homeostasis via the differentiation of hematopoietic stem cells (HSCs) [15]. Hematopoiesis occurs mainly in the red bone marrow in adults. In contrast to solid tumors, leukemia, especially acute myeloid leukemia (AML), has a relatively short latency period after exposure to ionizing radiation. Radiation-induced leukemia has an appreciably higher excess relative risk (ERR) than any of the other late-arising pathologies that have manifested within the A-bomb survivor cohort [16]. Therefore, the tissue weighting factor of red bone marrow has been set to 0.12 [4]. In this section, we focus on dose-rate effects on the hematopoietic system based on informative results from animal experiments.

Architecture, development and maintenance. The general features of the hematopoietic system in humans and mice have been well documented in ICRP 2012 [15] and 2015 [16] (Fig. 1). Briefly, the hematopoietic tissue is a hierarchical, self-renewing and cell-amplifying tissue, maintained by a very small number of stem cells and early progenitor cells that undergo asymmetric self-renewal following division cycles and differentiate into specific lineages, respectively. Differentiated blood cells include erythrocytes for oxygen transport, leukocytes for immune defense and platelets for hemostasis. A major site of hematopoiesis in the fetal stage is the liver and that in adults is the red bone marrow. Fetal liver HSCs undergo rapid cycling while HSCs of the adult bone marrow are quiescent. In mice, the gradual shift in the program governing HSCs cycling takes place approximately 3 weeks after birth.

Table 1. AOP and key events

1. Physical/chemical alterations
   - Ionization and excitation of macromolecules
   - Ionization of water molecules
2. Biochemical and molecular alterations
   - DNA damage induction
   - Chromatin damage induction
   - Epigenetic changes
3. Molecular and cellular responses
   - DNA damage repair and responses
     - Incorrect DNA damage repair
     - Generation of cancer driver mutations
   - Intra-cellular signaling
     - Mitochondria and nuclear DNA
   - Gene expression & protein production
   - Cell cycle regulation
   - Apoptosis, senescence-like cell death, autophagy, necrosis
   - Non-targeted effects and inter-cellular signaling
4. Tissue/organ responses
   - Disruption of structure and function of tissues/organs
   - Alteration of physiology and homeostasis
     - Stem and progenitor cells
     - Tissue clearance and stem cell competition
   - Inflammation and tissue remodeling
   - Alteration of tissue/organ developments
   - Development of premalignant regions
5. Adverse outcomes
   - Induction of cancer
   - Death from cancer

Quiescent HSCs in the steady-state marrow of humans and mice replicate at different rate, i.e. approximately 280 days and 145 days, respectively, suggesting that the number of replications of HSC through life is significantly different between species [16]. The daily turnover in the actively renewing cell system amounts to 490×10^9 cells in the hematopoietic renewal system in mice [17]. The average turnover rate of HSCs is ~2.5 weeks in mice (assessed by telomere shortening) [18, 19] and ~45 weeks in humans [18].

HSCs and multipotent hematopoietic progenitors (MPPs) can be isolated using various cell surface markers. In the adult mouse, all types of multipotent cells are contained in the c-Kit$^+$ Lineage$^{-/low}$Sca-1$^+$ (KLS) fraction of bone marrow cells. The KLS population includes CD34$^-$FLt3$^-$ long-term HSCs (LT-HSCs), which give rise to CD34$^+$FLt3$^-$ short-term HSCs (ST-HSCs) and then CD34$^+$FLT3$^+$ MPPs. HSCs and MPPs can be defined also by the expression levels of Thy-1, Mac-1 and CD4, i.e. HSCs are Thy-1^{low}Sca-1$^+$Lineage$^-$Mac-1$^-$CD4$^-$c-Kit$^+$, while MPPs are Thy-1^{low}Sca-1$^+$Lineage$^-$Mac-1^{low}CD4^{low} [20]. Additionally, HSCs can be isolated using SLAM family markers as CD150$^+$CD45$^-$ KLS cells, while MPPs are as CD150$^-$CD48$^-$ KLS cells [21]. LT-HSCs are the most primitive and quiescent cells, which are responsible for the long-term renewal and maintenance of hematopoiesis. ST-HSCs are somewhat quiescent with higher self-renewal potential and shorter-term responsibilities for repopulating precursor marrow niches. MPPs are heterogenous

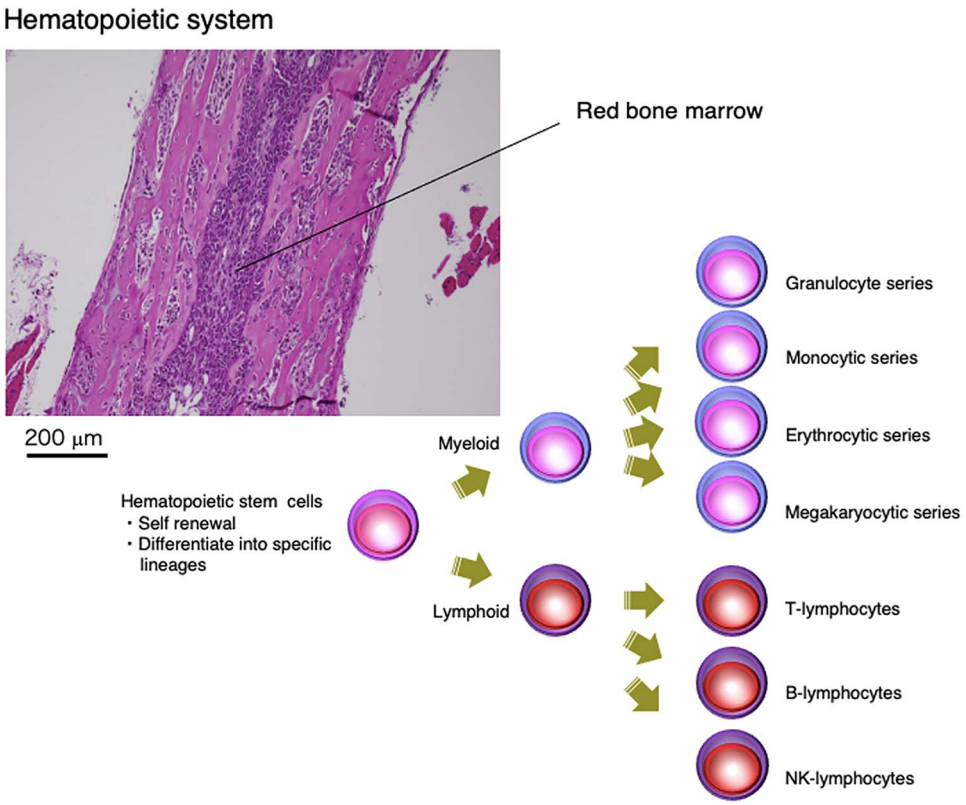

Fig. 1. Architecture of mouse bone marrow.

with respect to reconstitution kinetics in irradiated mice and the types of blood cells they can produce [16, 20]. The HSC niche in bone marrow is perivascular, created partly by mesenchymal stromal cells and endothelial cells and often, but not always, located near the trabecular bone [22].

An *in vitro* clonogenic assay showed that stem and progenitor cells (HSPCs: Sca-1^{+}CD34^{-}) were more radioresistant than common myeloid progenitors (CMP) and granulocyte/macrophage progenitors (GMPs), and Ataxia-telangiectasia mutated (ATM) is an essential mediator of this differential DNA damage response (DDR) [23]. Radiosensitivities of various murine HSCs and progenitor cell subsets are also reviewed in ICRP 2015 [16]. Primitive repopulating HSCs (marrow-repopulating ability [MRA] cells and cultured long-term repopulating initial cells [LTC-Ic]) are relatively radioresistant. Multipotential lineage-restricted spleen colony-forming cells (CFU-S), assayed on day 12 or 9, are less resistant. Granulocyte, erythroid, monocyte, megakaryocyte colony forming units (GEMM-CFU) and colony-forming unit-megakaryocyte (CFU-meg) are more resistant compared with erythroid-restricted progenitors, which are burst-forming units erythroid (BFUe) and colony-forming units erythroid (CFUe).

Dose-rate effect. Animal studies have shown that the hematopoietic system can maintain adequate cell numbers during chronic low dose and low dose-rate irradiation conditions [15] (Table 2). The influence of dose and dose rate on the life-shortening and oncogenic effectiveness of 1-MeV neutrons, 5-MeV neutrons, 250 kVp X-rays and ^{60}Co γ-rays was investigated in male and female RF/Un mice exposed to various doses of whole-body radiation at dose-rates of 10^{-8} to 1 Gy/min [24, 25]. In general, radiation-caused life shortening in 30-day survivors, which increased with increasing dose and dose rate at all levels of cumulative mortality [24]. Irradiated mice showed the same types of disease as did the controls, although the frequency, severity and age distribution of disease varied, depending on the dose, dose rate and radiation quality. In the continuously irradiated mice, dying within 1–4 months after the start of irradiation was observed at the highest dose-rate tested, and death was attributed to necrosis and aplasia of lymphatic and hemopoietic tissues with complicating hemorrhage and infection. The incidence of myeloid leukemia was markedly increased by acute exposure to all types of radiation tested, passing through a maximum at 2–4 Gy and declining at higher doses [25]. Chronic irradiation was less effective than acute irradiation for γ-rays; i.e. no leukemogenic effects were evident even after 2–3 Gy at the lowest dose rates, although chronic neutron irradiation seemed to be as effective as acute irradiation.

The effects of protracted whole-body exposure of beagles to ^{60}Co γ-rays were reported [26]. In those studies, the dogs were irradiated under two conditions: (i) continuous, duration-of-life exposures at dose rates of 0.0021–0.052 mGy/min; and (ii) discontinuous, fraction-of-life exposures at dose rates 0.026–0.18 mGy/min, with cumulative doses of 4.5–34.58 Gy and post-exposure times of 14–4702 days. Under continuous, duration-of-life exposure regimens, the overall

Table 2. Summary of animal studies comparing the effects of acute and chronic exposures on hematopoietic system

Species(strain)	Target of irradiation	Analysis	Radiation source	Dose, dose rate	Effect, continuous or fractionated	Effect, acute single	Reference
Mouse (RF/Un) Male Female 8–10 W	Whole body	Survival, incidence (until mice had accumulated predetermined total doses or 50% of the group had died)	X, 250 kVp	0–4.5 Gy (0.8 Gy/min) (Male)	**Life shortening** (Table V [24]) Mortality during exposure 0% ·11 days/Gy (Female) ·7.5 days/Gy (Male) Mortality during exposure ∼50% ·5 days/Gy (Female) ·3 days/Gy (Male)	**Life shortening** (Table V [24]) Mortality during exposure 0% ·33 days/Gy (Female) ·75 days/Gy (Male)	[24, 25]
					Myeloid leukemia induction (Table IX [25]) ·4%/Gy (Female, subchronic[a]) ·0.5%/Gy (Female, chronic[a]) **Thymic lymphoma induction** (Table IX [25]) ·3%/Gy (Female, subchronic[a]) ·1.5%/Gy (Female, chronic[a])	**Myeloid leukemia induction** (Table IX [25]) ·9%/Gy (Female) **Thymic lymphoma induction** (Table IX [25]) ·4%/Gy (Female)	
			γ, ^{60}Co	0–58.13 Gy (0.037–0.57 mGy/min) (Male) 0–98.75 Gy (0.004–67 mGy/min) (Female)			
			Fast neutrons, reactor, ^{210}Po-Be	0–3.32 Gy (1.2×10^{-3}–850 mGy/min) (Male) 0–9.3 Gy (3.0×10^{-5}–850 mGy/min) (Female)	**Life shortening** (Table V [24]) Mortality during exposure 0% ·87 days/Gy (Female) ·100 days/Gy Mortality during exposure ∼50% ·70 days/Gy (Female)	**Life shortening** (Table V [24]) Mortality during exposure 0% ·100 days/Gy (Female) ·80 days/Gy (Male)	
					Myeloid leukemia induction (Table IX [25]) ·7%/Gy (Female, subchronic[a]) ·8%/Gy (Female, chronic[a]) **Thymic lymphoma induction** (Table IX [25]) ·6%/Gy (Female, subchronic[a]) ·5%/Gy (Female, chronic[a])	**Myeloid leukemia induction** (Table IX [25]) ·6%/Gy (Female) **Thymic lymphoma induction** (Table IX [25]) ·4%/Gy (Female)	

(*Continued*)

Table 2. Continued

Species (strain)	Target of irradiation	Analysis	Radiation source	Dose, dose rate	Effect, continuous or fractionated	Effect, acute single	Reference
Dog (Beagle) Male Female 400–500 D	Whole body	Incidence (MPD), CFU-GM (duration of life (life span) or discontinuous, fraction-of-life exposure)	γ, ^{60}Co	Duration-of-life exposure regimens 11.13 ± 0.95 Gy (2.1×10^{-3} mGy/min) 26.57 ± 1.52 Gy (5.2×10^{-3} mGy/min) 38.05 ± 20.24 Gy (1.3×10^{-2} mGy/min) 50.96 ± 21.88 Gy (2.6×10^{-2} mGy/min) 49.22 ± 30.69 Gy (5.2×10^{-2} mGy/min) Discontinuous, fraction-of-life exposure regimens 0–15 Gy (2.6×10^{-2} mGy/min) 0–34.58 Gy (5.2×10^{-2} mGy/min) 0–15 Gy (8.9×10^{-2} mGy/min) 4.5 Gy (0.18 mGy/min)	**MPD** 1.4% (2.1×10^{-3} mGy/min) 41.7% (2.6×10^{-2} mGy/min) 45.5% (5.2×10^{-2} mGy/min)[b] 50.0% (8.9×10^{-2} mGy/min)[b] **CFU-GM** ∼6 mGy/mGy of daily dose rate (6.9×10^{-3}–5.2×10^{-2} mGy/min)[c] ∼61 mGy/mGy of daily dose rate (0–6.9×10^{-3} mGy/min)[c] **MPD** About 11% (total doses of 15–30 Gy at 5.2×10^{-2} mGy/min) About 5% (total doses of 4.5–10.5 Gy at 5.2×10^{-2} mGy/min) **CFU-GM** Ineffective in promoting (or maintaining) the radioresistance	- -	[26]
Dog (Beagle) Male Female 536 ± 27 D	Whole body	Incidence (MPD or AA[d]) (life span)	γ, ^{60}Co	0–83.71 ± 13.76 Gy (5.2×10^{-2} mGy/min)	**Marrow progenitor levels**[e] 91% (AA[d]-prone subgroup, <200 days) 95% (AA/PLS[f] variant, <200 days) ∼80% (MDP-prone subgroup, > 200 days) ∼115% (non-MPD-prone variant, > 200 days)	-	[27]

(*Continued*)

Table 2. Continued

Species (strain)	Target of irradiation	Analysis	Radiation source	Dose, dose rate	Effect, continuous or fractionated	Effect, acute single	Reference
Rat (August x Marshall F1)	Whole body	Survival, Hemopoietic response (until rats had accumulated predetermined total doses)	γ, ^{137}Cs	0.11–2.9 mGy/min	**Survival time days** 10 (2.9 mGy/min) 20 (1.2 mGy/min) 50 (0.58 mGy/min) 150–200 (0.35 mGy/min) $>$ 320 (0.11 mGy/min) **Fully hemopoietic system fails** $\geq$ 0.58 mGy/min (20 days at 1.2 mGy/min, $\leq$ 50 days (0.58 mGy/min))	-	[28, 29]
Dog (Beagle) Male Female 400–500 D	Whole body	Incidence (MPD, hemopoietic failure, tumor, or cell-producing capacity) (life span or discontinuous, fraction-of-life exposure)	γ, ^{60}Co	2.1×10^{-3}–0.44 mGy/min	**Death due to hemopoietic insufficiency** $\geq 1.3\times10^{-2}$ mGy/min hemopoietic failure (0.18, 0.26, 0.38 mGy/min) hemopoietic failure or MPD (2.6×10^{-2}, 5.2×10^{-2}, 8.8×10^{-2} mGy/min MPD (1.3×10^{-2} mGy/min)	-	[27, 28, 30–33]
Mouse (B6D2F$_1$) Male Female 3 M	Whole body	Survival ($LD_{50/30}$), CFU-S, CFU-F, CFU-GM) (life span or until mice had accumulated predetermined total doses)	X, 300 kVp γ, ^{137}Cs γ, ^{60}Co	700 mGy/min 4 Gy/min 0.5, 60 mGy/min	**Long-term recovery of CFU-S, CFU-F, CFU-GM** $\leq$ 12.5 Gy (γ, ^{60}Co, 0.5 Gy/min)	**Incomplete recovery of CFU-S, CFU-F, CFU-GM** $\leq$ 6.5 Gy (X, 300 kVp, $>$ 700 mGy/min) **$LD_{50/30}$** 6.7 Gy (X, 300 kVp) 7.8 Gy (γ, ^{137}Cs) 12.6 Gy (γ, ^{60}Co, 60 mGy/min)	[34]
Mouse (C57BL/6 J) Female 3–4 W	Whole body	Survival, incidence, Lymphocyte populations, Immunoglobulins (life span)	γ, ^{232}Th (shielding α-rays)	1.9×10^{-4} mGy/min	**Survival** [36] No difference **Incidence** [36] No difference: cancer, vascular disease and infections **Lymphocyte populations** [37] No difference: $CD4^+$, $CD8^+$ cells in the thymus and the spleen, or in the reactivity of T-cells to lectins **Immunoglobulins** [37] Significantly decreased: IgG1, IgG2b, IgG2a		[36, 37]

(*Continued*)

Table 2. Continued

Species (strain)	Target of irradiation	Analysis	Radiation source	Dose, dose rate	Effect, continuous or fractionated	Effect, acute single	Reference
Mouse (SJL/J) Female 3–4 W	Whole body	Survival, lymphocyte populations, Cell proliferation (Ki-67), Apoptosis (life span, until mice had accumulated a predetermined ages)	γ, ^{232}Th (shielding α-rays)	1.9×10^{-4} mGy/min	**Survival** [38] 417 days (397 days for controls) **Lymphocyte populations** [38] No difference: $CD3^+$, $CD4^+$ and $CD4^+CD25^+$ T cells and $CD79^+$ B cells in the spleen and lymph nodes Significantly decreased: cytotoxic $CD8^+$ T cells in lymph nodes (21.9 ± 1.9% for controls, 16.5 ± 1.4% for irradiated at 32 weeks) Slightly increased: $CD49^+$ NK cells in the spleen (ex. 0.33 ± 0.09% for controls, 0.62 ± 0.24% for irradiated at 32 weeks) **Cell proliferation (Ki-67)** [39] No difference at 32 weeks Significantly lower at 42 weeks (68.8 ± 13.3% for controls, 53.57 ± 5.3% for irradiated) **Apoptosis** [39] No difference	-	[38, 39]
Mouse (CBA-Ca) Male Female 7–9 W	Whole body (in utero)	Genomic instability (fMNCE, fMPCE) (average 16 days of foetal life)	γ, ^{137}Cs	0.7, 1.6, 4.2 Gy (3.1×10^{-2}, 6.9×10^{-2}, 0.18 mGy/min) * Female mice were irradiated during their pregnancy.	**Genomic instability** No delayed effects (higher fMPCE or fMNCE) Significant reduction of fMPCE was only found among the male offspring exposed at 0.18 mGy/min	-	[40]
Mouse (C57BL/6 J) Male 5 W	Whole body	Cell proliferation, gene expression in splenocyte (5 consecutive days/week for 2 [35] or 4 weeks [34])	γ, ^{60}Co	2.8×10^{-2}, 6.9×10^{-2} mGy/min (= 40, 100 mGy/day)	**Proliferative response to T cell mitogens**[g] [48] No difference: 100 mGy/day Significantly enhanced: 40 mGy/day **Proliferative response to anti-CD3** [49] Significantly enhanced: 40 mGy/day **Proliferative response to B cell mitogens**[h] [48] No difference: 40, 100 mGy/day **HSP70 mRNA, HSC70 and HSP72** [48] No difference: 100 mGy/day Elevated constitutive levels: 40 mGy/day **HSP70 mRNA and HSP72** [49] Elevated constitutive levels: 40 mGy/day	-	[48, 49]

(*Continued*)

Table 2. Continued

Species (strain)	Target of irradiation	Analysis	Radiation source	Dose, dose rate	Effect, continuous or fractionated	Effect, acute single	Reference
Rat (Wistar) Male (body weight 150–170 g)	Whole body	Synthetic activity of blood lymphocytes (until rats had accumulated 3 Gy)	γ, ^{137}Cs	3, 4, 7.5 Gy (2.27 Gy/min) $3.0\text{x}10^{-3}$, 7.6×10^{-3}, 1.5×10^{-2}, 0.1 mGy/min	**Change in synthetic activity (α_{mean})[i] during 3 months** $> 7.6\times10^{-3}$ mGy/min (the value ofα_{mean} decreased about 20% and 25% to the control level with a dose rate of 0.1 and 1.5×10^{-2} mGy/min, respectively.	**Change in synthetic activity (α_{mean})[i]** > 3 Gy	[51]
Mouse (C57BL/6 J) Male 1014 W	Whole body	HPRT mutation (until mice had accumulated predetermined total doses)	γ, ^{137}Cs	0–6 Gy (0.5 Gy/min, 0.69 mGy/min, 9.9×10^{-2} mGy/min)	**Mutant frequency of T cells (Linear fit)** $\alpha = (3.01 \pm 0.42)\ \text{x}10^{-6}$/Gy (0.69 mGy/min =1 Gy/day) $\alpha = (2.92 \pm 0.34)\ \text{x}10^{-6}$/Gy ($9.9\times10^{-2}$ mGy/min =1 Gy/week) **DDREF** ~1.5 (< 2 Gy, ≤ 1 Gy/day) 3–5 (higher doses)	**Mutant frequency of T cells** (0.5 Gy/min, Linear-quadratic fit) $\alpha = (6.86 \pm 5.21)$ $\text{x}10^{-6}$/Gy $\beta = (1.17 \pm 1.02)$ $\text{x}10^{-6}/\text{Gy}^2$ 0.5 Gy/min	[57]
Mouse (C3H/He Nrs) Male 8 W	Whole body	HSC with hemizygous deletion and point mutation of the *Sfpi* gene (until mice had accumulated 3 Gy)	γ, ^{137}Cs	1.4×10^{-2} mGy/min 0.14 mGy/min 1 Gy/min	**Estimated risk of rAML with PU.1 deficiency[j]** 0.17% (1.4×10^{-2} mGy/min) 0.72% (0.14 mGy/min)	**Estimated risk of rAML with PU.1 deficiency[j]** 1.9% (1 Gy/min)	[60]

[a]'subchronic' denotes that irradiation was terminated before and 'chronic' after appreciable mortality in the respective populations [25]; [b]eliminating the short-live dogs, i.e. dogs surviving less than 300 days, which represented 60.3% (5.2×10^{-2} mGy/min) and 73.3% (8.9×10^{-2} mGy/min) [26]; [c]GM progenitors of long-lived dogs (> 600 days) [26]; [d]AA, aplastic anemia [27]; [e]relative to the age-matched controls [27]; [f]AA/PLS, aplastic anemia/preleukemia syndrome [27]; [g]concanavalin A, phytohaemagglutinin and anti-CD3 [48]; [h]lipopolysaccharide [48]; [i]the parameterα representing the intensity ratio of emission bands in the red (I_{640nm}) and green (I_{530nm}) regions of the fluorescence spectrum in the cells stained with acridine orange [51]; [j]risk for HSCs to transform into PU.1-deficient rAML stem cells [60].

incidence of myeloproliferative disorders (MPD) increased from 1.4% at the lowest dose rate tested (3 mGy/day = 0.0021 mGy/min) to 41.7% at 0.026 mGy/min. At higher dose rates (0.052–0.18 mGy/min), the incidence of MPD declined concomitantly with a marked reduction in average survival time resulting from hematopoietically ablative hypoplastic/aplastic marrow diseases. On the other hand, the incidence of MPD continued to rise at the 0.052 and 0.089 mGy/min, reaching incidences of 45.5% and 50.0%, respectively, although there were short-live dogs, i.e. dogs surviving less than 300 days, which represented 60.3% of the group at 0.052 mGy/min and 73.3% of the group at 0.089 mGy/min. At the highest dose rate tested (0.18 mGy/min), all dogs exhibited ablative marrow responses to chronic exposure and associated short-term survival patterns (<300 days of survival) without any evidence of evolving MPD. Interestingly, a precipitous decline in the number of marrow CFU-GM (granulocyte/monocyte colony forming unit in agar) during the initial period of exposure (about 50–125 days) was followed by a gradual recovery to nearly control levels following extended periods of exposure (>700 days) in the long-lived, MPD-prone dogs continuously irradiated under 0.052 mGy/min. Under discontinuous, fraction-of-life exposure groups, the incidence of MPD was lower. Relatively low peaks of MPD incidence (about 11%) occurred at 0.052 mGy/min to total doses of 15 and 30 Gy. Incidences were further reduced (to about 5%) at lower cumulative doses (10.5 and 4.5 Gy), as well as at both lower (0.026 mGy/min) and higher (0.089 and 0.18 mGy/min) dose rates. However, there were individual differences in protracted irradiation at 0.052 mGy/min [27].

Fliedner *et al.* [28] reproduced the results that the effects of protracted irradiation of the blood forming organs of the rat examined first by Lamerton *et al.* in the 1950s [29]. Hematological responses in rats following continuous whole-body exposure to γ-rays were studied at dose-rates of 0.11, 0.35, 0.58 and 1.2 mGy/min. A lethal outcome was not observed at 0.11 and 0.35 mGy/min. After initial turbulences of cell counts, the hemopoietic system apparently could tolerate continuous irradiation at a certain level for some time individually before the hemopoietic system collapses. The organism tries to maintain homeostasis by increasing cell production to compensate for radiation-induced cell loss under chronic irradiation conditions. Meanwhile, the hemopoietic system failed fully within less than 20 days at 1.2 mGy/min and within about 50 days at 0.58 mGy/min. However, at this dose-rate, an initial short-lasting rise in peripheral blood cell counts turned to a decline to a minimum at approximately 20 days, followed by a small increase in all cell counts to a maximum at about 25 days, after which the system irreversibly tended to fail over the next 25 days. Additionally, the studies using the beagle dogs subjected to whole body ^{60}Co γ-rays irradiated continuously throughout life at relatively low dose-rates [27, 30, 31] were also reviewed [28]. The dose-rates to the whole body over the entire life span were 0.0021, 0.0052, 0.012, 0.026, 0.052 and 0.089 mGy/min. Higher dose-rates of 0.18, 0.26 and 0.44 mGy/min resulted in the death of all animals within 100 days. This is the largest systematic hematological chronic irradiation study known, where dogs were chronically exposed to radiation for their entire lifetime, i.e. until death occurred in the radiation field. Within the high dose-rate groups (0.38, 0.26 and 0.18 mGy/min) irradiation resulted in a lethal outcome caused by hemopoietic failure for all animals within a time span below 100 days of exposure. In the middle dose-rate groups (0.089, 0.052 and 0.026 mGy/min) there is a remarkable span in the survival times. For example, in the 0.089 mGy/min group the first death occurs after about 80 days of irradiation, the last death is observed after about 1000 days. The observed causes of death within the same dose group shift from hemopoietic insufficiency with septicemia and aplasia to MPD and fatal tumors. In the dose-rate group 0.013 mGy/min still some dogs died from MPD, but below this dose-rate the relative numbers of deaths from fatal tumors increased to the level seen in control dogs. In addition, there was no significant changes in the concentration of red blood cells, platelets and segmented granulocytes in the individual dogs in a clinically relevant way in the group of 92 dogs exposed to 0.0021 mGy/min (= 3 mGy/day) [30–32]. Fliedner *et al.* [28] summarized that canine studies show two major causes of death depending on dose-rate: hemopoietic failure and tumors. With decreasing low dose-rates, hemopoietic failure became infrequent and finally disappeared at about 0.0021 mGy/min. Then, tumors became the predominant fate at a near full life span, similar to the control unirradiated dogs. Trilineal cell-producing capacity (erythropoiesis, myelopoiesis and megakaryopoiesis) was also fully retained for several years of exposure at the lowest dose-rate tested (0.0021 mGy/min) but was completely lost within several hundred days at the highest dose-rate (0.18 mGy/min) [33].

There is a clear dose-rate effect of the $LD_{50/30}$ values of B6D2F1 mice; the values were about 6.7 Gy (300 kV X-rays, 700 mGy/min), 7.8 Gy (^{137}Cs γ-rays, 4 Gy/min) and 12.6 Gy (^{60}Co γ-rays, 60 mGy/min) [34]. Recovery of hemopoietic stem cells (CFU-S), CFU-GM and stromal colony-forming units (CFU-F) was almost complete by 1 year after doses up to 12.5 Gy at 0.5 mGy/min in comparison with incomplete recovery after only 6.5 Gy at >0.7 Gy/min. Importantly, the level of CFU-F recovery at 1 year after 6.5–12.5 Gy at 0.06 Gy/min was lower than the fully recovered after the same doses at 0.5 mGy/min, i.e. the DREF was 10 or more.

Female C57BL/6 J mice irradiated with γ-rays at 1.3×10^{-4} and 2.7×10^{-4} mGy/min (70 and 140 mGy/y, respectively) showed a significantly longer mean life span than controls [35]. Same group also studied using ^{232}Th γ-rays at 1.9×10^{-4} mGy/min (=100 mGy/y), no difference was observed in life-span, weigh curves or food intake between control and irradiated mice [36]. There was no adverse effect on malignant and non-malignant diseases. The percentage of $CD4^+$ and $CD8^+$ cells in the thymus and spleen, or in the reactivity of T-cells to lectins showed no difference between control and irradiated mice at 1.9×10^{-4} mGy/min [37]. While the number of B-cells in the spleen was unchanged, IgG1, IgG2b and IgG2a decreased significantly after 12, 18 and 24 months of irradiation, respectively. On the other hand, the SJL/J female mice irradiated with ^{232}Th γ-rays at 1.9×10^{-4} mGy/min (=100 mGy/y) showed slightly prolonged life span, i.e. the mean survival was 397 and 417 days for controls and irradiated mice, respectively [38]. The mice died of lymphoma. The percentages of $CD3^+$, $CD4^+$ and $CD4^+$-$CD25^+$ T cells and of $CD49^+$ B cells in the spleen and lymph nodes were not different between the irradiated and control groups, while cytotoxic $CD8^+$ T cells were significantly decreased in lymph nodes in irradiated mice. The percentages of $CD49^+$ NK cells were significantly Increased in

the spleens of Irradiated mice at 28 and 32 weeks, although NK cells activity remained unchanged.

Dose-rate effect of genomic instability in mice following prenatal irradiation with ^{137}Cs γ-rays was also studied [40]. Pregnant CBA/Ca mice were irradiated for an average of 16 days at dose rates of 0.031, 0.069 and 0.18 mGy/min. Peripheral blood was drawn from all offspring at 36 days after birth. Increased frequencies of micronucleated polychromatic erythrocytes (fMPCE) and/or micronucleated normochromatic erythrocytes (fMNCE) were not observed among the *in utero* exposed mice of either gender, although a significant reduction of fMPCE was detected among the male offspring exposed at 0.18 mGy/min. These results indicate that low dose-rate irradiated mice *in utero* did not induce damage in erythroid stem cells that can be detected as persistent or delayed chromosome aberrations.

Possible 'key events' related to dose rate effect in the hematopoietic system. Key events of the AOP related to dose-rate effect have been also unclear in the hematopoietic system as well as the digestive system. There are plenty of studies carried out at high dose and at a high dose-rate [15, 16], therefore, in this section we focused on the studies with the low dose-rate radiation effect and/or HSCs.

DNA damage responses. Sublethal damage (SLD) recovery of marrow CFU-GM from dogs irradiated with low dose-rate exposure to ^{60}Co γ-rays was studied [26]. Under continuous 0.052 mGy/min, the radiosensitivity to additional exposure to ^{60}Co γ-rays at 250 mGy/min to total doses between 0–3 Gy marrow CFU-GM from long-lived MPD-prone dogs changed markedly with both time of exposure and preclinical phase progression. During the initial phase of exposure (<100 days), marrow CFU-GM from these dogs exhibited a high degree of radiosensitivity (D_0 ~500 mGy), whereas following extended exposure periods (>300 days), progenitors exhibited markedly Increased levels of radioresistance (D_0 ~1.5 Gy). The capacity of progenitor's SLD repair declined from the high levels observed for dog irradiated at 0.052 mGy/day to control-like levels at 0.013 mGy/min. At the lower dose-rate (0.052 to 0 mGy/min), the SLD repair capacity again was substantially elevated at 0.052 mGy/min relative to the controls. An extended survey of the radioresistance progenitor phenotype within the marrow of long-lived dogs showed that discontinuous, fraction-of-life exposure regimens were largely ineffective for promoting (or maintaining) the radioresistance. Only those dogs irradiated at the relatively high dose-rate of 0.088 mGy/min and doses of 10.5 and 15 Gy were moderately radioresistant. Dose rates (< 0.088 mGy/min), as well as the lower cumulative doses, consistently failed to elicit (or maintain) levels of radioresistance comparable to those observed under continuous irradiation.

DSB repair-related genes have essential roles for quality control of HSCs and/or their progenitors. Endogenous DNA damage accumulated with age in wild-type HSCs, and their proliferating progenitors could repair more readily or eliminate accumulating DNA damage [41]. Ito *et al.* [42] first reported that ATM serves essential roles in the reconstitutive capacity of HSCs but is not important for the proliferation or differentiation of progenitors, in a telomere-independent manner in mice. Atm knockout mice older than 24 weeks showed progressive bone marrow failure caused by a loss of function of HSCs associated with elevated ROS. Elevation of ROS induces HSC-specific phosphorylation of p38 MAPK accompanied by a defect in the maintenance of HSC quiescence [43]. Additionally, HSCs harvested from old mice exhibit diminished ATM activity and attenuated DNA damage response (DDR), leading to elevated clonal survival in response to a range of genotoxins, including ionizing radiation, that was underwritten by diminished apoptotic priming [44]. Interestingly, when HSCs from old mice were transplanted into young recipients, ATM signaling and clonal survival in response to DNA damage could be restored to the levels observed in young HSCs. This observation indicates that the defect in DDR of old HSCs was non-cell autonomous.

Canonical-NHEJ (c-NHEJ)-related Ku80 [41], DNA-PKcs [45], and DNA ligase IV [46, 47] and are also critical for the maintenance of HSCs. Competitive transplantation of LT-HSCs from *Ku80*$^{-/-}$ mice showed that *Ku80*$^{-/-}$ LT-HSCs were unable to generate mature B and T cells as a result of an inability to undergo V(D)J recombination, and were also impaired in their ability to reconstitute myeloid lineages [41]. The DNA ligase IV mutant (*Lig4*^{Y288C}) mouse is the viable model of human LIG4 syndrome [46]. The *Lig4*^{Y288C} mutation causes progressive loss of HSCs and cellularity of bone marrow with age. The *Lig4*^{Y288C} mutation also causes multiple defects in lymphocyte survival and proliferation, and in B cell class switch recombination [47]. Knock-in mice with the *DNA-PKcs*$^{3A/3A}$ allele, which codes for three alanine substitution at the mouse Thr2605 phosphorylation cluster (Thr2605, Thr2634 and Thr2643), die prematurely because of congenital bone marrow failure [45]. Loss of proliferative activity of *DNA-PKcs*$^{3A/3A}$ HSC s mainly caused by accumulation of DNA damage following Trp53-dependent apoptosis. Furthermore, *DNA-PKcs*$^{3A/3A}$ mouse embryo fibroblasts (MEFs) showed hypersensitivity not only to ionizing radiation but also to DNA cross-linking agents, and they were also defective in HR, and the Fanconi anemia DDR pathways as well as c-NHEJ.

Gene expression. Splenocytes from male C57BL/6 J mice irradiated with ^{60}Co γ-rays at 2.8×10^{-2} mGy/min (40 mGy/day) showed elevated constitutive levels of HSP70 mRNA, HSC70 and HSP72 [48]. Splenocytes could respond to T cell antigens by further increasing levels of those and by mounting a heightened proliferative response, although exposure to 0.069 mGy/min (0.10 Gy/day) was ineffective. In addition, T cells of mice irradiated at 0.028 mGy/min (40 mGy/day/exposure/day, 5 consecutive days/week, 2 weeks) showed elevated constitutive levels of Hsp70 mRNA and HSP72, and they responded to T-cell receptor-specific anti-CD3 stimulation by producing more Hsp70 mRNA and HSP72 and by proliferating more extensively than T cells of controls [49].

Cell death. In SJL/J female mice irradiated with ^{232}Th γ-rays at 1.9×10^{-4} mGy/min (=100 mGy/y), the mean values of percentages of Ki-67^{+} cell nuclei in lymphomatous lymph nodes did not change at 32 weeks but significantly lower at 42 weeks than controls [39]. On the other hand, the percentage of apoptotic bodies were not significantly changed between irradiated and control mice.

Intercellular signaling. Thrombopoietin (TPO) and its receptor Mpl are master regulators of both megakaryopoiesis and HSCs. TPO increases HSC interaction with the osteoblastic niche and to support HSC quiescence and expansion. TPO stimulates DNA repair both *in vitro* and *in*

vivo by increasing DNA-PK-dependent c-NHEJ, suggesting that niche factors can modulate the HSC DSB repair machinery [50].

Alteration of physiology and homeostasis. As described above, the precipitous decline in the number of marrow CFU-GM during the initial period of exposure (approximately 50–125 days) was followed by a gradual recovery to nearly control levels following extended periods of exposure (>700 days) in the long-lived, MPD-prone dogs continuously irradiated under 0.052 mGy/min [26]. Data accumulated by Fliedner *et al.* [28] are compatible with the 'injured stem cell hypothesis,' that radiation–injured stem cells, depending on dose-rate, may continue to deliver clones of functional cells that maintain homeostasis of hemopoiesis throughout life. Following whole-body exposure of rats to γ-rays at 0.35 mGy/min, the initial response was a short lasting rise in peripheral blood cell counts within the first days of exposure [29]. This was followed by a decline in cell counts to a minimum again at approximately 20 days. Thereafter, the system appeared capable of reestablishing homeostasis with some cell count undulations during the 200 days of observation. The early temporary rise was hardly seen at 0.11 Gy/min when the initial drop in cell counts reached a minimum at approximately 20 days followed by recovery to a cell count plateau of homeostasis, again with some cell count oscillations during the 300 days of observation. It is the hypothesis that the remarkable capacity of recovery at 0.35 and 0.11 mGy/min is, nevertheless, accompanied by some functional deficit that may appear in the cell count oscillations. This presumed deficit may be indicative of cell kinetic adaptations in the pool of stem cells, all of which must carry damage that possibly is distributed stochastically in the stem cell pool, thus giving rise to injured stem cell clones.

Systemic activity of blood lymphocytes is also affected by dose rate [51]. After high dose-rate irradiation (2.27 Gy/min), the synthetic activity of rat blood lymphocytes decreased sharply, indicating the predominant damaging effect. On the contrary, the synthetic activity increased by the stimulatory effect of low-dose radiation during the first four stages after starting irradiation under continuous irradiation conditions (0.1 mGy/min).

Fliedner and Graessle [52] also estimated the 'excess cell loss' using the data of the beagles [27, 31, 32] applying the biomathematical models [53, 54]. Excess cell loss was found to increase with increasing daily dose rate from the rate of $\varepsilon^* = 0.0011$/h at a dose rate of 0.0021 mGy/min (= 3 mGy/day) to a rate of $\varepsilon^* = 0.0123$/h at a dose rate of 0.0088 mGy/min, where ε^* denotes the fraction of cells lost per hour from the compartment. As described above, hemopoietic failure became infrequent and finally disappeared at about 0.0021 mGy/min. At the same rates of excess cell loss, the content of the model stem cell compartment was greatly reduced than the content of the thrombocyte compartment. Drawn from this fact is that cell numbers of the hematopoietic progenitor and stem cell pools, especially in the case of pluripotent stem cells, are affected by radiation-induced excess cell loss to a much greater extent than that recognized by the platelet counts in the peripheral blood.

Radiation-induced stem cell competition was first identified in HSCs by Bonder and Medzhitov [55], as well as the stem cells of the small intestine [56], while it has not been proved under low dose-rate irradiation conditions. To assess stem cell competition [55], bone marrow was harvested 4 days after 1 Gy of irradiation to exclude direct proapoptotic effects on competing cells. Bone marrow cells from irradiated mice were transferred into lethally irradiated recipient mice, either alone or mixed with untreated competitor cells. The percentage of HSPCs from untreated donors increased about 4-hold relative to their initial 10% in the injected cell mixture. Stem cell competition involved long-term repopulating stem cells, because it affected multiple lineages as well as phenotypic HSCs as late as 16 weeks post-transplantation. HSPCs from the unirradiated donor replaced a significant number of HSPCs from irradiated wild-type donor, but not from irradiated *Trp53*$^{+/-}$ donor mice. Additionally, stem cell competition may be mediated by non-cell-autonomous induction of growth arrest and senescence-related gene expression in outcompeted cells with higher Trp53 activity.

Development of premalignant lesions and dose-rate effect. The frequency of hypoxanthine phosphoribosyl transferase (HPRT)-deficient splenic T lymphocytes was measured in mice irradiated with ^{137}Cs γ-rays by the T cell cloning method [57]. Radiation-induced mutant frequency depended markedly on dose, dose-rate and time after exposure. When mutant fractions were determined 8 ~ 10 weeks after high dose-rate irradiation (500 mGy/min), the dose-effect curve fitted to the linear-quadratic equation. However, the dose-effect data could be fitted by linear equation in low dose-rate experiments at 0.69 and 0.099 mGy/min (1 Gy/day and 1 Gy/week, respectively). When low dose-rate-irradiated mice were dissected 30 ~ 40 weeks after irradiation, the value of mutant frequency was about one-third of that observed after 8 weeks. For doses <2 Gy the DDREF was ~1.5 when dose-rate was ≤1 Gy/day, whereas the DDREF was 3–5 at higher doses.

Radiation-induced acute myeloid leukemia (rAML) is commonly seen in humans and mice, and large hemizygous deletions on chromosome 2 (Chr2) around the *Sfpi1* (*PU.1*) allele in the rAML cells were Identified in more than 80% of mice [58, 59]. Hirouchi *et al.* [59] found that the CD-antigen profiles and gene expression profiles of rAML stem cells were similar to those of CMPs and that there was continuous proliferative stress on HSCs, MPPs and CMPs. They suggested that hemizygous deletion of *Dusp2* on Chr2 contributed to the self-renewal potential of rAML stem cells, and the initial rAML stem cell may originate not only from irradiated stem cells but also from MPPs and CMPs [16, 59]. Recently, Ojima *et al.* [60] studied the dose-rate dependence of the frequency of hemizygous deletion of the *Sfpi1* gene (*DSG*) and point mutation of the allele *Sfpi1* gene (*PMASG*) in HSCs of C3H mice received a total dose of 3 Gy of ^{137}Cs γ-rays at 0.014, 0.14 (20, 200 mGy/day), or 1000 mGy/min. They found that frequency of HSCs with the *DSG* was proportional to dose rate. Additionally, immunofluorescent analysis of both *Sfpi1* (*PU.1*) and GM-CSF receptor-α also showed the dose-rate-dependent levels of *Sfpi1* (*PU.1*)-inactivated HSCs. They suggested a mechanism for dose-rate dependent rAML as follows: (i) radiation-induce DNA damage in HSCs in a dose-rate dependent manner, and the subsequent *DSG* occurring at an early stage during the DDR; (ii) HSCs with DNA damage and/or *DSG* are outcompeted by normal HSCs; and (iii) cell proliferation is to recover the number of HSCs decreased by radiation. These results indicate a dose-rate effect on mutagenesis and suggest a dose-rate-dependent induction of hematopoietic tumors.

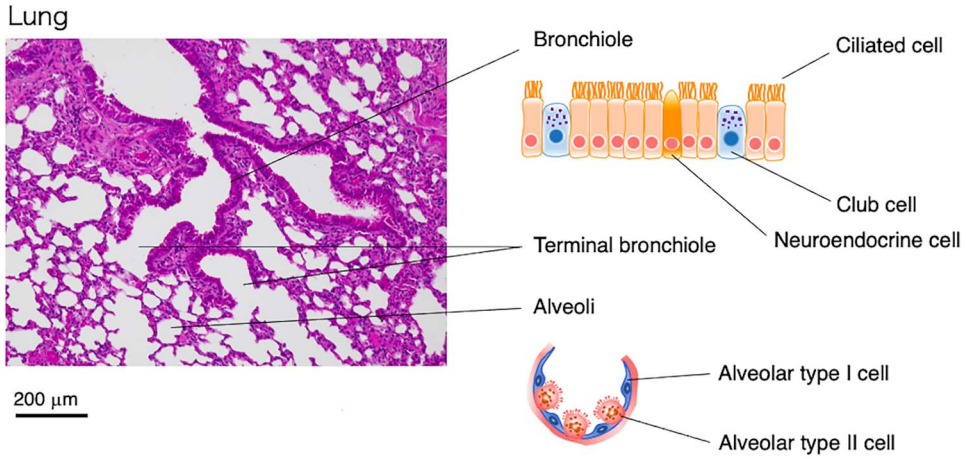

Fig. 2. Architecture of mouse lung.

Lung

Lung cancer is one of the most common types of cancer and its prognosis is poor in the majority of cases. The risk of lung cancer is greater for men than for women, and cigarette smoking is the leading risk factor [61]. Epidemiological evidence from the Life Span Study of atomic bomb survivors demonstrated that radiation also increases the risk of lung cancer [61]. As with many other solid cancers, the ERR/Gy decreases with attained age, however, the risk of lung cancer increases with the increasing of the age at exposure.

Architecture, development and maintenance. The lung is a respiratory organ essential for breathing and responsible for gas exchange between air and blood. Under normal physiological conditions, cell turnover in the adult lung is slower than that of other organs such as the skin and intestine [62, 63]. However, substantial repair and regeneration may take place in lung tissue after insult or injury [64–66]. The mature lung comprises four main biologically distinct portions: the trachea, bronchi, bronchioles and alveoli. The trachea and larger bronchi are lined with a pseudostratified epithelium composed of basal and luminal cells. The more distal bronchiolar region is lined with an epithelium monolayer consisting of secretory (Club; formerly known as Clara), ciliated and neuroendocrine epithelial lineages (Fig. 2). The alveoli are located in the alveolar sacs of the lungs, where gas exchange occurs. The alveoli are composed of type I and type II alveolar epithelial cells, capillaries and various resident mesenchymal cells including myofibroblasts and lipofibroblasts. Alveolar type I (AT1) cells cover ~95% of the alveolar surface; they exhibit an expanded flattened morphology and are responsible for gas exchange between the alveoli and blood. Alveolar type II cells (AT2 cells) are cuboidal in morphology and contain secretory granular organelles known as lamellar bodies that fuse with the cell membrane thus mediating secretion of pulmonary surfactant (Fig. 2).

Lung development is divided into three main periods, namely: embryonic, fetal and postnatal lung development period called alveolization, which continues until young adulthood [67]. Alveologenesis requires the proliferation and differentiation of epithelial progenitors in coordination with the mesenchyme [67].

Dose-rate effect on radiation carcinogenesis. Studies on radiation-induced lung cancer in mice have produced somewhat conflicting results regarding the dose-rate effect on lung carcinogenesis (Table 3). Notably, mice of different strains show highly variable sensitivity to radiation-induced lung tumor, as well as the incidence of spontaneous tumor [68]. The fact that lung cancer is a late-onset disease in mice further complicates the studies of radiation carcinogenesis. Thus, the incidence of other early-onset cancers hinders analysis of the dose-rate effect of radiation on lung cancer. Also, the competition among the cause of death should be considered.

In humans, radiation-induced lung cancer risk increases with increasing age at exposure. Based on this knowledge, it can be assumed that the value of DREF might also depend on this factor. However, review of the available reports from rodent models gives limited information on this issue. Besides, most of them did not apply low dose-rate radiation. While Sasaki reported that the incidence of lung cancer decreased with increasing age at exposure in B6C3F1 female mice [69, 70], Yamada *et al.* reported that Wistar rats subjected to thoracic irradiation at 5 or 15 weeks of age showed increased rates of lung adenocarcinoma compared with those irradiated at 1 week of age [71]. Ullrich *et al.* reported that the incidence of lung adenomas by neutron radiation at 12 weeks of age was higher than that at 25 weeks of age [72]. Despite these studies, the mechanisms of radiation-induced carcinogenesis remain to be elucidated, and it is also important to understand the dose-rate dependence of cancer induction.

Possible 'key events' related to dose-rate effect in the lung. In the last 10 years advanced techniques, such as cell-lineage tracing, single-cell RNA sequencing and organoid culture combined with injury models have provided novel information about the multiple stem/progenitor cell populations in different regions of the adult lung. In the proximal airways, basal cells are a population of multipotent stem cells that drive both homeostasis of the normal epithelium and its regeneration after injury. In the distal bronchiolar region, secretoglobin family 1a member 1-expressing club cells can self-renew and retain differentiation capacity. Stem cell populations were also identified at the bronchoalveolar duct junction (BADJs) [86–88]. In the adult lung alveolus,

Table 3. Lung carcinogenesis induced by acute or chronic radiation

Mouse	Exposure type	Analysis	Radiation source	Dose, dose rate	Effect	Reference
RFMf/Un Female 12 W	Whole body	Incidence*	γ, ^{137}Cs	0–300 rad, 45 rad/min	Decreased incidence with increased dose except at approximately 300 rad	[72]
RFMf/Un Female Male 10 ± 0.5 W	Whole body	Incidence	γ, ^{137}Cs	0–300 rad, 45 rad/min	Decreased incidence with increased dose over the range 10 to 100 rad increased incidence at 300 rad	[73]
RFMf/Un Female 10 ± 0.5 W	Whole body	Incidence	γ, ^{137}Cs	0–200 rad (40 rad/min) 0–200 rad (0.0069 rad/min)	No increase	[74]
RF/Un Female Male 8-10 W	Whole body	Incidence	X rays γ, ^{137}Cs	Female 0–750 rad (6.7 rad/min) 0–9875 rad (0.0004–0.0739 rad/min) Male 0–450 rad (80 rad/min) 0–5813 rad (0.0037 rad/min-0.0570 rad/min)	No increase	[76]
RFM/Un Female 10-12 W	Thoracic	Incidence, Tumor number/ mice (at 9 months after irradiation)	X rays	0–900 rad (400 rad/min) 0–900 rad (400 rad/min) two equal fractions separated by 24 hr 0–900 rad (400 rad/min) two equal fractions separated by 30 days	Increase of dose dependent tumor number per mouse Single: linear dose-squared model with a shallow positive initial slope, or threshold model with a dose-squared region above the threshold Fraction: linear model	[77, 78]
SAS/4 Female	Whole body	Incidence	γ, ^{60}Co	0–4 Gy (1.0 Gy/min) 0–4 Gy (1.67 mGy/min)	Increased incidence dose dependently at both dose rate Reduction in effectiveness of low dose rate: 3–4	[79]
BALB/c/An NBdf Female 10 ± 0.5 W	Whole body	Incidence	γ, ^{137}Cs	0–200 rad (40 rad/min) 0–200 rad (0.0069 rad/min)	Increased incidence dose dependently at both dose rates The ratio of slope: 1.9	[74]
BALB/c/An NBd Female 12 W	Whole body	Incidence	γ, ^{137}Cs	0–200 rad (40 rad/min) 0–200 rad (0.0069 rad/min)	High dose rate: Linear or linear-quadratic response Low dose rate: Linear model with a slope similar to the linear portion of the high-dose-rate linear-quadratic response	[75, 80]

(*Continued*)

Table 3. Continued

Mouse	Exposure type	Analysis	Radiation source	Dose, dose rate	Effect	Reference
B6C3F1 Female Day7	Whole body	Incidence, excess relative risk, age at death	γ, ^{137}Cs	0–0.95 Gy (0.8 Gy/min)	Excess relative risk: 0.3 ± 0.29 at 0.1 Gy, 2.21 ± 1.01 at 0.48 Gy, 3.14 ± 1.43 at 0.95 Gy, Incidence: increased dose dependently Age at death: earlier dose dependently	[81]
B6CF1 Male 110 ± 7 days	Whole body	Incidence	γ, ^{60}Co	0–49 Gy Low dose rate ($\leq$ 0.08 mGy/min)	Full dose range LDEF at high dose rate (95%CI) 0.758 (0.667, 0.874) LDEF at low dose rate (95%CI) 0.982 (0.637, 2.392) DREF (95%CI) 1.403 (0.878, 3.843) Dose restriction ≤5Gy LDEF at high dose rate (95%CI) 0.890 (0.503, 2.215) LDEF at low dose rate (95%CI) -2.654 (−13.175, 9.875) DREF (95%CI) -3.185 (−16.729, 11.047)	[82–85]

B6C3F1: C57BL/6JNrs and C3H/HeNrs
B6CF1: C57BL/6JNrs and BALB/cJAnl
* Incidence (until mice died or were moribund)

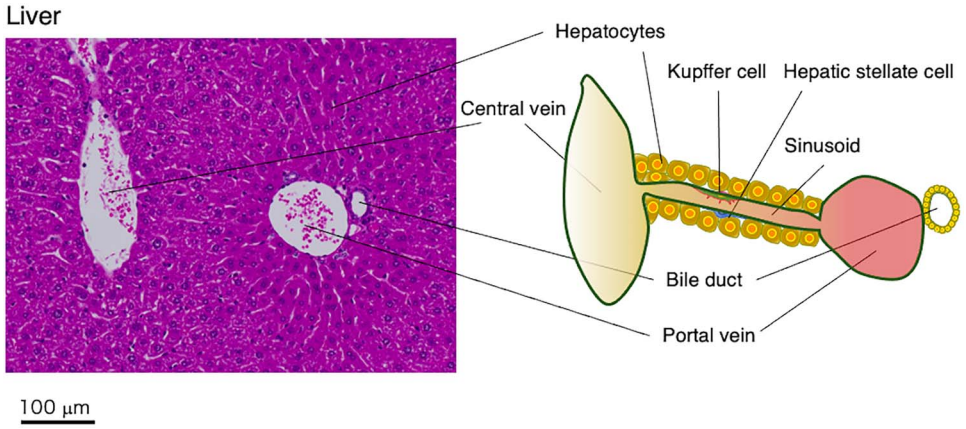

Fig. 3. Architecture of mouse liver.

surfactant protein C-positive (SFTPC-positive) AT2 cells function as alveolar progenitors and long-term stem cells and can give rise to AT1 cells [62, 63]. Oncogenic *Kras*^{G12D} expression in AT2 cells can efficiently generate multifocal clonal adenomas [63]. Several reports have characterized lung mesenchymal cells [89, 90]. Lgr6-expressing cells or Axin2-positive cells were found surrounding bronchiolar epithelia and in the alveolar space, whereas Lgr5-expressing cells were mostly identified in the alveolar niche. These mesenchymal cell types in the lung influence epithelial homeostasis and regeneration through serving stem cell niche.

Thus, in distinct regions of the lung different populations of epithelial cells function as adult stem/progenitor cells. Interestingly, these stem/progenitor cells are not undifferentiated, and they express genes associated with specialized functions. Under certain circumstances such as tissue injury, these stem/progenitor cells display remarkable lineage plasticity and can change their phenotype by 'de-differentiation,' consequently giving rise to different cell types. The pathways for maintenance of stemness and regeneration may manifest diversity depending on the stem/progenitor cells. For instance, it was reported that in the proximal airways, Notch signaling is active in steady state airways and increase during repair. Notch is required for differentiation, but not self-renewal of basal cells [91, 92]. In the proximal region of the lung, AT2 stem cells require Wnt signaling from neighboring single-cell fibroblast niches, whereas in the alveolar region of the lung injury induces autocrine Wnt that transiently expand the progenitor pool [93].

Recent studies are starting to provide exciting insights into how the stem cell compartment operates during not only normal homeostasis of the lung, but also in the development of radiation-induced lung cancer. For example, in the bronchiolar region of the mouse lung, *in vivo* irradiation was shown to cause a reduction in clonogenicity and to promote expansion of the remaining progenitors to replace the damaged tissue [94, 95]. It was also reported that lung basal stem cells rapidly repaired radiation-induced DNA damage using the pathway of NHEJ [96].

In conclusion, even though we have solid evidence to believe that stem/progenitor cells and stem cell niches are crucial players in tumor development, the key events in the AOP related to dose-rate effects in the lung remain largely unknown. Further extensive experiments are needed to elucidate these pathways in distinct regions of the lung and bronchial tree, and to address the issue of dose-rate effects in the lung.

Liver

Tissue architecture, development and maintenance. Liver tissue contains various types of cells, such as hepatocytes, bile duct epithelial cells, Kupffer cells, sinusoid endothelial cells and hepatic stellate cells (HepSCs) (Fig. 3). Liver has long been known as a highly regenerative organ, however, the source of cells for new hepatocytes after liver injury has also been debated for a long time [97]. While several types of liver stem cells have been identified, the plasticity of hepatocytes and biliary epithelial cells was also involved in liver regeneration [98]. Thus, the liver stem cells involved in tissue damage repair after radiation is still to be determined.

Dose-rate effect on radiation carcinogenesis. Since hepatocellular carcinoma is the major type of cancer in liver, hepatocytes and their progenitor cells should be a cell origin of liver cancer. While liver is the major organ-at-risk for radiation-induced carcinogenesis, an insufficient number of studies have directed to elucidate the mechanism of radiation-induced liver cancer.

Development of liver neoplasms following radiation exposure has been known for many years (Table 4). In early studies, hepatoma induction was demonstrated with either single or fractionated radiation exposure [99, 100], and its age-dependency was also observed [101]. For example, (C57L x A) F1 mice, referred to as LAF1, were exposed to γ-rays or X-rays at 280 to 300 mGy/min, and overall incidence for hepatoma was 2% for doses ranging from 2.6 Gy to 11 Gy, while the baseline incidence was 6% [102, 103]. LAF1 mice were also exposed to radiation from an atomic bomb explosion (mostly γ-rays), and observed incidence for benign hepatoma and malignant hepatoma was 5.54% and 0.16% for the control groups, and 9.21% and 0.48% for the γ-irradiated groups, respectively [99]. In large-scale experiments using female RFM/Un mice exposed to γ-rays at 450 mGy/min, increased incidence of liver tumors was not detectable with doses between 0.1 and 3 Gy [73].

In other experiments, (C57BL/6 x C3H) F1 mice were exposed to X-rays at 0.35 Gy/min at 1, 15 and 42 days of age, and the effects

Table 4. Liver tumors induced by acute and chronic radiation

Mouse strains (Age at exposure)	Radiation exposure	Endpoint of analysis	Radiation source	Dose (dose rate)	Effect	Reference
RFMf/Un (10 ± 0.5 W)	Whole body	Incidence	γ, ^{137}Cs	0.1–3 Gy, (0.45 Gy/min)	Little increase in liver tumor incidence	[73]
C57BL/6 x C3H F1 (Day 1, 15, 42)	Whole body	Hepatoma incidence	X, 230 kV, 25 mA	2–4 fractionation of 2.8 Gy (320 R) (0.35 Gy/min (40 R/min))	Hepatoma incidence at 86 weeks: 18% (2.8 Gy x1) 28% (0.7 Gy x4)	[101]
C57BL/Cne x C3H/HeCne (4-6 W)	Whole body	Incidence	X, 250 kV	0.04–2.56 Gy (0.06 Gy/min. 0.68 Gy/min)	No clear dose-dependence in hepatoma incidence	[106]
C57BL/6NCrj x C3H/HeNCrj (6 W)	Whole body	Incidence	X, 250 kVp, 25 mA	0.5, 5.0 Gy (0.1 Gy/min, 1 Gy/min)	No clear induction of hepatoma	[108]
C57BL/6JNrs x C3H/HeNrs (1 W)	Whole body	Incidence	γ, ^{137}Cs	0.1, 0.48, 0.95 Gy (0.8 Gy/min)	ERR—0.21 at 0.10 Gy ERR = 7.32 at 0.48 Gy ERR = 12.59 at 0.95 Gy	[81]
B6C3F1 (8 W)	Whole body	Incidence	γ, ^{137}Cs	0.02, 0.4, 8 Gy (0.05, 1.1, 21 mGy/day (22 h))	Incidence of adenoma: 15.5%/0 mGy 22.2%/0.05 mGy/day 22.4%/1.1 mGy/day 23.2%/21 mGy/day Incidence of carcinoma: 29.3%/0 mGy 34.3%/0.05 mGy/day 31.2%/1.1 mGy/day 27.7%/21 mGy/day	[110]

of fractionated exposure were examined. The results indicated significant age-dependent decrease in the frequency of hepatoma only in the male mice [101]. Similar results were obtained by the study, in which (C57BL/Cne × C3H/HeCne) F1 male mice were exposed to various doses of X-rays at 133 mGy/min *in utero*, at 3 and 19 months. Liver tumors were rarely induced at 19 months [104]. It was indicated that radiation exposure tended to shorten the latency period for hepatoma induction [99]. Accelerated hepatoma development was clearly observed in neonatal (C57BL/6JNrs × WHT/Ht) F1 (B6WF1) mice exposed to 1.75–5.26 Gy of X-rays at 480–530 mGy/min [105].

In the subsequent studies, dose–response for the induction of hepatoma was further determined. For example, one study using (C57BL/Cne x C3H/HeCne) F1 (BC3F1) and CBA/Cne mice exposed to X-rays at 1.26 to 1.34 Gy/min showed that X-irradiation with 3 Gy or more significantly increased an incidence of hepatoma, but exposure to 7 Gy gave the incidence lower than that of the control value [106]. The same group also investigated the hepatoma incidence in BC3F1 mice exposed to 40 mGy - 2.56 Gy of X-rays at 60 mGy/min and 680 mGy/min for lower and higher doses, respectively, and they did not find clear dose-dependent hepatoma induction at lower doses, while the incidence of overall solid cancers showed dose-dependent increase [107, 108]. A similar conclusion was obtained in the study using (C57BL/6NCrj x C3H/HeNCrj) F1 (B6C3F1) mice exposed to X-rays with 0.5 and 5.0 Gy exposed at 100 mGy/min [109].

Details of the dose–response relationship for induction of liver tumors has been described lately in (C57BL/6JNrs x C3H/HeNrs) F1 (B6C3F1) neonatal mice exposed to 480 mGy to 5.7 Gy of γ-rays at 870 mGy/min [110]. The results demonstrated that the induction of liver cancer increased with increasing dose up to 3 Gy, while it slightly decreased at higher doses. Age-dependency of liver tumor incidence was also examined by the same group, in which mice were irradiated at day 17 of the intra-uterine period, or at days 0, 7, 35, 105 and 365 of the postnatal periods. Significantly higher incidence of liver tumors was observed at days 0 (53.8%) and 7 (54.9%) after birth, while incidence was only 19.7% for the control group [70], indicating that low dose and dose-rate effects must be affected by age at exposure.

Accordingly, the effects of low dose were examined at day 7 postnatal age. Although an early study, in which mice were irradiated at 4 to 6 weeks of age did not show any increase in hepatoma incidence below 1 Gy of X-rays [106], B6C3F1 mice exposed to doses below 1 Gy of γ-rays at 0.8 Gy/min at 7 days of age showed increased liver tumor incidence with 480 mGy and 950 mGy, but not with 100 mGy [81].

In an early study, LAF1 mice were exposed to 6.18 Gy to 24 Gy of γ-rays at 0.24 mGy/min, and the hepatoma incidence was reported to be 32% in contrast to the 6% for the control mice [100]. The Institute for Environmental Sciences (IES) in Japan conducted a series of studies was conducted with 400 days' chronic exposures at very low-dose-rate, including 0.05 mGy/day, 1 mGy/day and 20 mGy/day, until the

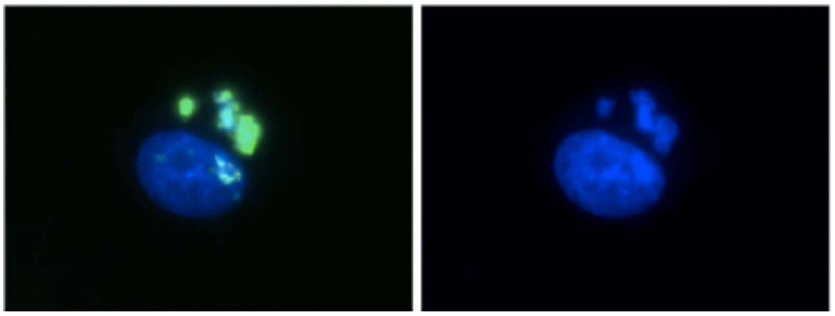

Fig. 4. Apoptosis in micronuclei. Human mammary epithelial cells (HMEC) were exposed to 10 Gy of γ-rays, and incubated for 24 h. Fixed cells were stained with anti-phosphorylated histone H2AX at serine 139 and Alexa488-conjugated secondary antibody. Micronuclei stained with DAPI (right) show homogeneous staining with anti-phosphorylated H2AX antibody (left), indicating that apoptosis is executed only in the micronuclei.

total doses reached to 20 mGy, 400 mGy and 8 Gy, respectively. The study demonstrated that the incidence of liver tumors was increased in the 20 mGy/day group examined [111, 112]. The increased ratio was approximately 2-fold, which was slightly lower than the approximately 3-fold in mice exposed at 0.87 Gy/min [110].

Genetically engineered mice should be good tools for defining radiation effects, and one study, using *FHIT* KO mice, demonstrated that 1 Gy exposed at 1 Gy/min increased the incidence of liver cancer, while 1 Gy delivered in 10 fractions (100 mGy daily for 10 days) did not show such an increase [113].

Possible 'key events' related to dose-rate effect. With respect to the key events, studies using C57BL/6 J and B6C3F1 mice chronically exposed to low-dose γ-rays reported changes in expressions of the genes [114, 115]. Differential protein expression was also reported in the C57BL/6 J mice exposed to 20 mGy/day, and they were different from those detected at a high dose rates (720 mGy/min or 550 mGy/min) [116]. Proteomics analysis was also performed with C57BL/6 J mice exposed to γ-rays for 90 days at a dose rate of 0.05 to 1 mGy/h, demonstrating modulation of proteins related to stress response, such as calreticulin and GSTP1 [117, 118]. Furthermore, a recent study demonstrated protein markers associated with liver adenoma induced by low-dose-rate radiation [119].

Altered metabolism could also be the one pathway worth further consideration [120, 121]. For example, it has been demonstrated that low-dose-rate radiation exposure accelerates fatty liver reaction [122]. It was reported that not only high-dose-rate exposure but also low-dose-rate exposure accelerated fatty liver [122]. Moreover, an unexpected link between liver cancer and obesity-associated intestinal microbial metabolism was reported recently [123]. Obesity changes the spectrum of microbiota, which results in enhanced metabolism of bile acid, generating deoxycholic acid (DCA) and lipoteichoic acid (LTA). These metabolites are harmful to HepSCs and induce senescence-like cell death through the production of DSBs. Then, senesced HepSCs secreted factors that promote cancer development. It was also showed that secreted factors from HepSC contained prostaglandin (PG) E2, which mediates suppression of CD8+ T cell activity [124].

Besides the functional analyses of HepSCs [125], different types of stem cells existed in different parts of liver tissue were studied [126, 127]. Insult-dependent roles are expected for these different types of stem cells [128], but their role after radiation exposure is still an open question.

In order to bring the knowledge obtained in animal experiments back to human epidemiology, it will be necessary to identify physiological difference in the liver tissue between animals and humans. Also, species differences in the stem cell biology have to be determined. Together with such information it should enable extrapolation of knowledge from animal experiments to humans.

NOVEL KEY EVENTS TO BE INTEGRATED IN THE AOP TO DOSE-RATE EFFECTS

In addition to the nuclear DDR, an unexpected role of exo-nuclear signaling was demonstrated. Previously, histone H2AX phosphorylation was reported in micronuclei [129], indicating caspase-dependent apoptotic fragmentation (Fig. 4). Recent evidence has revealed that cytoplasmic fragmented DNA executes an innate immune response through activation of the cGAS-STING pathway [130], which resulted in secretion of cytokines, such as interleukin (IL)-1β, IL-6, and tumor necrosis factor (TNF)-α [130]. They were involved in cellular senescence and senescence-associated phenotypes [131]. Because micronuclei induction is dose-rate dependent [132], the resultant induction of inflammation and senescence could also be dose-rate dependent, which might be a new important key event for dose-rate effects.

Senescence-associated secretory phenotype (SASP) was originally described in senesced cultured cells, and its impact on cancer development has been discussed in depth [133]. It has been recognized that SASP could modify tissue microenvironment in response to radiation exposure [134]. It was found that many SASP factors are exactly the same as so-called bystander factors, such as TNF-α, IL-1 and IL-8 [135].

In relation to the senescence-associated inflammatory response, or the radiation-induced inflammation overall [136], other novel key event emerging should be radiation effect on the immune response. In fact, the possible involvement of immunosenescence in cancer risk was discussed in a study of A-bomb survivors [137].

Although the influence of the microenvironment on radiation carcinogenesis has not been well understood except in the mammary gland [138], the kinetics of stem cells greatly relies on the local microenvironment [16]. Thus, a tissue-based response, which is specific for liver, should be another key event to be integrated into

AOP. For example, at least two types of stem cells are known to exist in the liver, one near the central vein and the other in the portal vein, so that differences in radiosensitivity must be taken into account.

SUMMARY AND THE FUTURE PERSPECTIVES

Current review compiles animal studies with respect to the dose-rate effect, and discusses the results with regard to the underlying biological mechanisms. As a result, it became clear that our knowledge is still far from the full representation of low-dose-rate effects. Thus, studies using experimental animal models are compelled to adopt innovative *in vivo* research tools to facilitate consolidation of our understanding of the underlying mechanisms of tissue/organ reactions, which result in adverse outcomes.

From this point of view, indispensable role of tissue response must be emphasized. For example, long-term exposure of low-dose-rate radiation could be influenced by the kinetics of DSB repair and tissue turnover, as well as by age-related physiological changes of the tissues/organs. In addition, it is indispensable to provide a bridge that fills the gap between epidemiological studies and experimental animal studies. In the current review, several mechanisms underlying the dose-rate effect in animal models were provided, which will make it possible to assess whether a common mechanism is applicable to human tissues/organs. Comparison of the biological differences between animals and humans should provide a clue to promote better understanding of the results obtained from the different species.

ACKNOWLEDGMENTS

This work was conducted as a part of the activity of Planning and Acting Network for Low Dose Radiation Research (PLANET). We are also grateful to the following members of the administration committee and the working group of PLANET who are not the authors of the present work: Drs. Kotaro Ozasa, Toshiyasu Iwasaki, Kazuo Sakai, Takashi Sugihara, Junya Kobayashi, Hiroshi Tauchi, Hiroshi Yasuda and Shin-ichi Kudo. We thank Drs. Yoshiya Shimada, Kazuo Yoshida, Michiya Sasaki, Tetsuo Nakajima and Daisuke Iizuka for their insightful comments and support.

DATA AVAILABILITY

The data underlying this article will be shared on reasonable request to the corresponding author.

CONFLICT OF INTEREST

The authors confirm they have no conflicts of interest.

REFERENCES

1. UNSCEAR 2013. Levels and effects of radiation exposure due to the nuclear accident after the 2011 great east-Japan earthquake and tsunami. *UNSCEAR 2013 Report. Volume I, Scientific annex A*, pp. 1–311. New York: United Nations, 2014.
2. Ozasa K. Epidemiological research on radiation-induced cancer in atomic bomb survivors. *J Radiat Res* 2016;57:i112–7.
3. Grant EJ, Brenner A, Sugiyama H *et al.* Solid cancer incidence among the life span study of atomic bomb survivors: 1958–2009. *Radiat Res* 2017;187:513–37.
4. ICRP 2007. *The 2007 Recommendations of ICRP. Publication 103. Ann ICRP 2007*;37:1–332. New York: Elsevier, 2007.
5. Brooks AL, Hoel DG, Preston RJ. The role of dose rate in radiation cancer risk: evaluating the effect of dose rate at the molecular, cellular and tissue levels using key events in critical pathways following exposure to low LET radiation. *Int J Radiat Biol* 2016;92:405–26.
6. Ruhm W, Woloschak GE, Shore RE *et al.* Dose and dose-rate effects of ionizing radiation: a discussion in the light of radiological protection. *Radiat Environ Biophys* 2015;54:379–401.
7. Ruhm W, Azizova T, Bouffler S *et al.* Typical doses and dose rates in studies pertinent to radiation risk inference at low doses and low dose rates. *J Radiat Res* 2018;59:ii1–ii10.
8. Haley BM, Paunesku T, Grdina DJ *et al.* The increase in animal mortality risk following exposure to sparsely ionizing radiation is not linear quadratic with dose. *PLoS One* 2015;10:e0140989.
9. Tang FR, Loke WK, Khoo BC. Low-dose or low-dose-rate ionizing radiation-induced bioeffects in animal models. *J Radiat Res* 2017;58:165–82.
10. Paunesku T, Haley B, Brooks A *et al.* Biological basis of radiation protection needs rejuvenation. *Int J Radiat Biol* 2017;93:1056–63.
11. Paunesku T, Woloschak G. Reflections on basic science studies involving low doses of ionizing radiation. *Health Phys* 2018;115:623–7.
12. Helm JS, Rudel RA. Adverse outcome pathways for ionizing radiation and breast cancer involve direct and indirect DNA damage, oxidative stress, inflammation, genomic instability, and interaction with hormonal regulation of the breast. *Arch Toxicol* 2020. https://doi.org/10.1007/s00204-020-02752-z.
13. Chauhan V, Sherman S, Said Z *et al.* A case example of a radiation-relevant adverse outcome pathway to lung cancer. *Int J Radiat Biol* 2020;97:68–84. https://doi.org/10.1080/09553002.2019.1704913.
14. UNSCEAR 2012. *Biological Mechanisms of Radiation Actions at Low Doses. UNSCEAR 2012 Report*. pp. 1–35. New York: United Nations, 2012.
15. ICRP, 2012. *ICRP Statement on Tissue Reactions/Early and Late Effects of Radiation in Normal Tissues and Organs – Threshold Doses for Tissue Reactions in a Radiation Protection Context*. ICRP Publication 118. Ann ICRP 2012;41(1/2).
16. Niwa O, Barcellos-Hoff MH, Globus RK *et al.* ICRP. ICRP publication 131: stem cell biology with respect to carcinogenesis aspects of radiological protection. *Ann ICRP* 2015;44:7–357.
17. Fliedner TM, Steinbach KH, Hoelzer D. Adaptation of environmental changes: the role of cell-renewal systems. In: Finck ES (ed). *The Effects of Environment on Cells and Tissues: Excerpta Medica*. Amsterdam: Wolters Kluwer, 1976, 20–38.
18. Shepherd BE, Guttorp P, Lansdorp PM *et al.* Estimating human hematopoietic stem cell kinetics using granulocyte telomere lengths. *Exp Hematol* 2004;32:1040–50.

19. Shepherd BE, Kiem HP, Lansdorp PM *et al.* Hematopoietic stem-cell behavior in nonhuman primates. *Blood* 2007;110: 1806–13.
20. Morrison SJ, Weissman IL. The long-term repopulating subset of hematopoietic stem cells is deterministic and isolatable by phenotype. *Immunity* 1994;1:661–73.
21. Kiel MJ, Yilmaz OH, Iwashita T *et al.* SLAM family receptors distinguish hematopoietic stem and progenitor cells and reveal endothelial niches for stem cells. *Cell* 2005;121:1109–21.
22. Morrison SJ, Scadden DT. The bone marrow niche for haematopoietic stem cells. *Nature* 2014;505:327–34.
23. Mohrin M, Bourke E, Alexander D *et al.* Hematopoietic stem cell quiescence promotes error-prone DNA repair and mutagenesis. *Cell Stem Cell* 2010;7:174–85.
24. Upton AC, Randolph ML, Conklin JW. Late effects of fast neutrons and gamma rays in mice as influenced by the dose rate of irradiation: life shortening. *Radiat Res* 1967;32:493–509.
25. Upton AC, Randolph ML, Conklin JW. Late effects of fast neutrons and gamma-rays in mice as influenced by the dose rate of irradiation: induction of neoplasia. *Radiat Res* 1970;41:467–91.
26. Seed TM, Kaspar LV. Acquired radioresistance of hematopoietic progenitors (granulocyte/monocyte colony-forming units) during chronic radiation leukemogenesis. *Cancer Res* 1992;52: 1469–76.
27. Seed TM, Meyers SM. Chronic radiation-induced alteration in hematopoietic repair during preclinical phases of aplastic anemia and myeloproliferative disease: assessing unscheduled DNA synthesis responses. *Cancer Res* 1993;53:4518–27.
28. Fliedner TM, Graessle DH, Meineke V, Feinendegen LE. Hematopoietic response to low dose-rates of ionizing radiation shows stem cell tolerance and adaptation. *Dose Response* 2012;10:644–63.
29. Lamerton LF, Pontifex AH, Blackett NH *et al.* Effects of protracted irradiation on the blood-forming organs of the rat. Part 1: continuous exposure. *Br J Radiol* 1960;33:287–301.
30. Fritz TE, Tolle DV, Doyle DE *et al.* Hematologic responses of beagles exposed continuously to low doses of 60Co-gamma radiation. In: Baum SJ, Ledney GD, Thierfelder S (eds). *Experimental Hematology Today*. Basel: Karger, 1982, 229–40.
31. Fritz TE, Seed TM, Tolle DV *et al.* Late effects of protracted whole body irradiation by ^{60}Co gamma rays. In: Thompson RC, Mahaffey IA (eds). *Life-Span Radiation Effects Studies in Animals: What Can they Tell us?: United States Department of Energy*. Washington DC, 1986, 116–41.
32. Fritz TE. The influence of dose, dose rate and radiation quality on the effect of protracted whole body irradiation of beagle. In: Fliedner TM, Feinendegen LE, Hopewell JW (eds). *Chronic Irradiation: Tolerance and Failure in Complex Biological Systems: British Institute of Radiology*. London, 2002, 103–13.
33. Seed TM, Fritz TE, Tolle DV *et al.* Hematopoietic responses under protracted exposures to low daily dose gamma irradiation. *Adv Space Res* 2002;30:945–55.
34. Gallini R, Hendry JH, Molineux G *et al.* The effect of low dose rate on recovery of hematopoietic and stromal progenitor cells in gamma-irradiated mouse bone marrow. *Radiat Res* 1988;115:481–7.
35. Caratero A, Courtade M, Bonnet L *et al.* Effect of a continuous gamma irradiation at a very low dose on the life span of mice. *Gerontology* 1998;44:272–6.
36. Courtade M, Billote C, Gasset G *et al.* Life span, cancer and non-cancer diseases in mouse exposed to a continuous very low dose of gamma-irradiation. *Int J Radiat Biol* 2002;78: 845–55.
37. Courtade M, Caratero A, Jozan S *et al.* Influence of continuous, very low-dose gamma-irradiation on the mouse immune system. *Int J Radiat Biol* 2001;77:587–92.
38. Lacoste-Collin L, Jozan S, Cances-Lauwers V *et al.* Effect of continuous irradiation with a very low dose of gamma rays on life span and the immune system in SJL mice prone to B-cell lymphoma. *Radiat Res* 2007;168:725–32.
39. Lacoste-Collin L, Jozan S, Pereda V *et al.* Influence of a continuous very low dose of gamma-rays on cell proliferation, apoptosis and oxidative stress. *Dose Response* 2015;13:1–17.
40. Abramsson-Zetterberg L, Zetterberg G, Sundell-Bergman S *et al.* Absence of genomic instability in mice following prenatal low dose-rate gamma-irradiation. *Int J Radiat Biol* 2000;76: 971–7.
41. Rossi DJ, Bryder D, Seita J *et al.* Deficiencies in DNA damage repair limit the function of haematopoietic stem cells with age. *Nature* 2007;447:725–9.
42. Ito K, Hirao A, Arai F *et al.* Regulation of oxidative stress by ATM is required for self-renewal of haematopoietic stem cells. *Nature* 2004;431:997–1002.
43. Ito K, Hirao A, Arai F *et al.* Reactive oxygen species act through p38 MAPK to limit the lifespan of hematopoietic stem cells. *Nat Med* 2006;12:446–51.
44. Gutierrez-Martinez P, Hogdal L, Nagai M *et al.* Diminished apoptotic priming and ATM signalling confer a survival advantage onto aged haematopoietic stem cells in response to DNA damage. *Nat Cell Biol* 2018;20:413–21.
45. Zhang S, Yajima H, Huynh H *et al.* Congenital bone marrow failure in DNA-PKcs mutant mice associated with deficiencies in DNA repair. *J Cell Biol* 2011;193:295–305.
46. Nijnik A, Woodbine L, Marchetti C *et al.* DNA repair is limiting for haematopoietic stem cells during ageing. *Nature* 2007;447:686–90.
47. Nijnik A, Dawson S, Crockford TL *et al.* Impaired lymphocyte development and antibody class switching and increased malignancy in a murine model of DNA ligase IV syndrome. *J Clin Invest* 2009;119:1696–705.
48. Nogami M, Huang JT, James SJ *et al.* Mice chronically exposed to low dose ionizing radiation possess splenocytes with elevated levels of HSP70 mRNA, HSC70 and HSP72 and with an increased capacity to proliferate. *Int J Radiat Biol* 1993;63: 775–83.
49. Nogami M, Huang JT, Nakamura LT *et al.* T cells are the cellular target of the proliferation-augmenting effect of chronic low-dose ionizing radiation in mice. *Radiat Res* 1994;139:47–52.
50. de Laval B, Pawlikowska P, Petit-Cocault L *et al.* Thrombopoietin-increased DNA-PK-dependent DNA repair limits hematopoietic stem and progenitor cell mutagenesis in response to DNA damage. *Cell Stem Cell* 2013;12:37–48.

51. Karnaukhova NA, Sergiyevich LA, Aksenova GY *et al.* Synthetic activity of rat blood lymphocytes under acute and continuous gamma-irradiation -fluorescent microspectral study. *Radiat Environ Biophys* 1999;38:49–56.
52. Fliedner TM, Graessle DH. Hematopoietic cell renewal systems: mechanisms of coping and failing after chronic exposure to ionizing radiation. *Radiat Environ Biophys* 2008;47:63–9.
53. Graessle DH. (2002) Mathematical modelling of the blood platelet renewal system as an approach to analysing the effects of chronic irradiation on haematopoiesis. In: Fliedner TM, Feinendegen LE, Hopewell JW (eds). *Chronic Irradiation: Tolerance and Failure in Complex Biological Systems: British Institute of Radiology*. London, 2002, 202–7.
54. Hofer EP, Bruecher S, Mehr K *et al.* (1995) an approach to a biomathematical model of lymphcoytopoiesis. *Stem Cells* 1995;13:290–300.
55. Bondar T, Medzhitov R. p53-mediated hematopoietic stem and progenitor cell competition. *Cell Stem Cell* 2010;6:309–22.
56. Fujimichi Y, Otsuka K, Tomita M *et al.* An efficient intestinal organoid system of direct sorting to evaluate stem cell competition in vitro. *Sci Rep* 2019;9:20297.
57. Lorenz R, Deubel W, Leuner K *et al.* Dose and dose-rate dependence of the frequency of HPRT deficient T lymphocytes in the spleen of the ^{137}Cs gamma-irradiated mouse. *Int J Radiat Biol* 1994;66:319–26.
58. Rithidech K, Dunn JJ, Roe BA *et al.* Evidence for two commonly deleted regions on mouse chromosome 2 in gamma ray-induced acute myeloid leukemic cells. *Exp Hematol* 2002;30:564–70.
59. Hirouchi T, Akabane M, Tanaka S *et al.* Cell surface marker phenotypes and gene expression profiles of murine radiation-induced acute myeloid leukemia stem cells are similar to those of common myeloid progenitors. *Radiat Res* 2011;176:311–22.
60. Ojima M, Hirouchi T, Etani R *et al.* Dose-rate-dependent PU.1 inactivation to develop acute myeloid leukemia in mice through persistent stem cell proliferation after acute or chronic gamma irradiation. *Radiat Res* 2019;192:612–20.
61. Cahoon EK, Preston DL, Pierce DA *et al.* Lung, laryngeal and other respiratory cancer incidence among Japanese atomic bomb survivors: an updated analysis from 1958 through 2009. *Radiat Res* 2017;187:538–48.
62. Barkauskas CE, Cronce MJ, Rackley CR *et al.* Type 2 alveolar cells are stem cells in adult lung. *J Clin Invest* 2013;123:3025–36.
63. Desai TJ, Brownfield DG, Krasnow MA. Alveolar progenitor and stem cells in lung development, renewal and cancer. *Nature* 2014;507:190–4.
64. Basil MC, Katzen J, Engler AE *et al.* The cellular and physiological basis for lung repair and regeneration: past, present, and future. *Cell Stem Cell* 2020;26:482–502.
65. Hogan BL, Barkauskas CE, Chapman HA *et al.* Repair and regeneration of the respiratory system: complexity, plasticity, and mechanisms of lung stem cell function. *Cell Stem Cell* 2014;15:123–38.
66. Kotton DN, Morrisey EE. Lung regeneration: mechanisms, applications and emerging stem cell populations. *Nat Med* 2014;20:822–32.
67. Schittny JC. (2017). Development of the lung. *Cell Tissue Res* 2017;367:427–44.
68. Wakamatsu N, Devereux TR, Hong HH *et al.* (2007). Overview of the molecular carcinogenesis of mouse lung tumor models of human lung cancer. *Toxicol Pathol* 2007;35:75–80.
69. Sasaki S. Influence of the age of mice at exposure to radiation on life-shortening and carcinogenesis. *J Radiat Res* 1991;32:73–85.
70. Sasaki S, Fukuda N. Temporal variation of excess mortality rate from solid tumors in mice irradiated at various ages with gamma rays. *J Radiat Res* 2005;46:1–19.
71. Yamada Y, Iwata KI, Blyth BJ *et al.* Effect of age at exposure on the incidence of lung and mammary cancer after thoracic X-ray irradiation in Wistar rats. *Radiat Res* 2017;187:210–20.
72. Ullrich RL, Jernigan MC, Cosgrove GE *et al.* The influence of dose and dose rate on the incidence of neoplastic disease in RFM mice after neutron irradiation. *Radiat Res* 1976;68:115–31.
73. Ullrich RL, Storer JB. Influence of gamma irradiation on the development of neoplastic disease in mice. *II Solid tumors. Radiat Res* 1979;80:317–24.
74. Ullrich RL, Storer JB. Influence of gamma irradiation on the development of neoplastic disease in mice. *III Dose-rate effects. Radiat Res* 1979;80:325–42.
75. Ullrich RL, Jernigan MC, Satterfield LC *et al.* Radiation carcinogenesis: time-dose relationships. *Radiat Res* 1987;111:179–84.
76. Upton AC, Randolph ML, Conklin JW *et al.* Late effects of fast neutrons and gamma-rays in mice as influenced by the dose rate of irradiation: induction of neoplasia. *Radiat Res* 1970;41:467–91.
77. Ullrich RL, Jernigan MC, Adams LM. Induction of lung tumors in RFM mice after localized exposures to X rays or neutrons. *Radiat Res* 1979;80:464–73.
78. Ullrich RL. Effects of split doses of x rays or neutrons on lung tumor formation in RFM mice. *Radiat Res* 1980;83:138–45.
79. Coggle JE. The role of animal models in radiation lung carcinogenesis. *Radiat Environ Biophys* 1991;30:239–41.
80. Ullrich RL. Tumor induction in BALB/c female mice after fission neutron or gamma irradiation. *Radiat Res* 1983;93:506–15.
81. Sasaki S, Fukuda N. Dose-response relationship for life-shortening and carcinogenesis in mice irradiated at day 7 postnatal age with dose range below 1 Gy of gamma rays. *J Radiat Res* 2006;47:135–45.
82. Tran V, Little MP. Dose and dose rate extrapolation factors for malignant and non-malignant health endpoints after exposure to gamma and neutron radiation. *Radiat Environ Biophys* 2017;56:299–328.
83. Thomson JF, Williamson FS, Grahn D *et al.* Life shortening in mice exposed to fission neutrons and gamma rays I. single and short-term fractionated exposures. *Radiat Res* 1981;86:559–72.
84. Thomson JF, Williamson FS, Grahn D *et al.* Life shortening in mice exposed to fission neutrons and gamma rays II. Duration-of-life and long-term fractionated exposures. *Radiat Res* 1981;86:573–9.
85. Thomson JF, Grahn D. Life shortening in mice exposed to fission neutrons and gamma rays. VIII. Exposures to continuous gamma radiation. *Radiat Res* 1989;118:151–60.

86. Kim CF, Jackson EL, Woolfenden AE *et al.* Identification of bronchioalveolar stem cells in normal lung and lung cancer. *Cell* 2005;121:823–35.
87. Lee JH, Bhang DH, Beede A *et al.* Lung stem cell differentiation in mice directed by endothelial cells via a BMP4-NFATc1-thrombospondin-1 axis. *Cell* 2014;156:440–55.
88. Salwig I, Spitznagel B, Vazquez-Armendariz AI *et al.* Bronchioalveolar stem cells are a main source for regeneration of distal lung epithelia in vivo. *EMBO J* 2019;38:e102099.
89. Lee JH, Tammela T, Hofree M *et al.* Anatomically and functionally distinct lung mesenchymal populations marked by Lgr5 and Lgr6. *Cell* 2017;170:1149–63.
90. Zepp JA, Zacharias WJ, Frank DB *et al.* Distinct mesenchymal lineages and niches promote epithelial self-renewal and myofibrogenesis in the lung. *Cell* 2017;170:1134–48.
91. Rock JR, Gao X, Xue Y *et al.* Notch-dependent differentiation of adult airway basal stem cells. *Cell Stem Cell* 2011;8:639–48.
92. Giuranno L, Wansleeben C, Iannone R *et al.* NOTCH signaling promotes the survival of irradiated basal airway stem cells. *Am J Physiol Lung Cell Mol Physiol* 2019;317:L414–L23.
93. Nabhan AN, Brownfield DG, Harbury PB *et al.* Single-cell Wnt signaling niches maintain stemness of alveolar type 2 cells. *Science* 2018;359:1118–23.
94. Farin AM, Manzo ND, Kirsch DG *et al.* Low- and high-LET radiation drives clonal expansion of lung progenitor cells in vivo. *Radiat Res* 2015;183:124–32.
95. McConnell AM, Konda B, Kirsch DG *et al.* Distal airway epithelial progenitor cells are radiosensitive to high-LET radiation. *Sci Rep* 2016;6:33455.
96. Weeden CE, Chen Y, Ma SB *et al.* Lung basal stem cells rapidly repair DNA damage using the error-prone nonhomologous end-joining pathway. *PLoS Biol* 2017;15:e2000731.
97. Kopp JL, Grompe M, Sander M. Stem cells versus plasticity in liver and pancreas regeneration. *Nat Cell Biol* 2016;18:238–45.
98. Li W, Li L, Hui L. Cell plasticity in liver regeneration. *Trend Cell Biol* 2020;30:329–38.
99. Upton AC, Kimball AW, Furth J *et al.* Some delayed effects of atom-bomb radiations in mice. *Cancer Res* 1960;20:1–60.
100. Nowell PC, Cole LJ. Hepatoma in mice: incidence increased after gamma irradiation at low dose rates. *Science* 1965;148:96–7.
101. Vesselinovitch SD, Simmons EL, Mihailovich N *et al.* The effect of age, fractionation, and dose on radiation carcinogenesis in various tissues of mice. *Cancer Res* 1971;31:2133–42.
102. Nowell PC, Cole LJ. Late effects of fast neutrons versus X-rays in mice: nephrosclerosis, tumors, longevity. *Radiat Res* 1959;11:545–56.
103. Cole LJ, Nowell PC. Late effects of fractionated X-irradiation in mice. Failure to prevent nonthymic lymphomas by thigh-shielding. *Radiat Res* 1963;18:487–94.
104. Di Majo V, Coppola M, Rebessi S *et al.* Age-related susceptibility of mouse liver to induction of tumors by neutrons. *Radiat Res* 1990;124:227–34.
105. Sasaki S, Kasuga T. Life-shortening and carcinogenesis in mice irradiated neonatally with X rays. *Radiat Res* 1981;88:313–25.
106. Di Majo V, Coppola M, Rebessi S *et al.* Radiation-induced mouse liver neoplasms and hepatocyte survival. *J Natl Cancer Inst* 1986;77:933–9.
107. Covelli V, Coppola M, Di Majo V *et al.* Tumor induction and life shortening in BC3F1 mice at low doses of fast neutrons and X rays. *Radiat Res* 1988;113:362–74.
108. Covelli V, Coppola M, Di Majo V *et al.* The dose-response relationships for tumor induction after high-LET radiation. *J Radiat Res* 1991;32:110–7.
109. Watanabe H, Ogiu T, Nishimura M *et al.* Comparison of tumorigenesis between accelerated heavy ion and X-ray in B6C3F1 mice. *J Radiat Res* 1998;39:93–100.
110. Sasaki S, Fukuda N. Dose-response relationship for induction of solid tumors in female B6C3F1 mice irradiated neonatally with a single dose of gamma rays. *J Radiat Res* 1999;40:229–41.
111. Braga-Tanaka I 3rd, Tanaka S, Ichinohe K *et al.* Cause of death and neoplasia in mice continuously exposed to very low dose rates of gamma rays. *Radiat Res* 2007;167:417–37.
112. Braga-Tanaka I 3rd, Tanaka S, Kohda A *et al.* Experimental studies on the biological effects of chronic low dose-rate radiation exposure in mice: overview of the studies at the Institute for Environmental Sciences. *Int J Radiat Biol* 2018;94:423–33.
113. Yu X, Lu L, Wen S *et al.* The effects of Fhit on tumorigenesis after multi-exposure to low-dose radiation. *Int J Clin Exp Med* 2009;2:348–53.
114. Uehara Y, Ito Y, Taki K *et al.* Gene expression profiles in mouse liver after long-term low-dose-rate irradiation with gamma rays. *Radiat Res* 2010;174:611–7.
115. Vares G, Uehara Y, Ono T *et al.* Transcription factor-recognition sequences potentially involved in modulation of gene expression after exposure to low-dose-rate γ-rays in the mouse liver. *J Radiat Res* 2011;52:249–56.
116. Nakajima T, Wang B, Ono T *et al.* Differences in sustained alterations in protein expression between livers of mice exposed to high-dose-rate and low-dose-rate radiation. *J Radiat Res* 2017;58:421–9.
117. Yi L, Li L, Yin J *et al.* Proteomics analysis of liver tissues from C57BL/6J mice receiving low-dose ^{137}Cs radiation. *Environ Sci Pollut Res* 2016;23:2549–56.
118. Yi L, Hu N, Yin J *et al.* Up-regulation of calreticulin in mouse liver tissues after long-term irradiation with low-dose-rate gamma rays. *PLoS One* 2017;12:e0182671.
119. Sugihara T, Tanaka S, Braga-Tanaka I 3rd *et al.* Screening of biomarkers for liver adenoma in low-dose-rate γ-ray-irradiated mice. *Int J Radiat Biol* 2018;94:315–26.
120. Nakajima T, Ninomiya Y, Nenoi M. Radiation-induced reactions in the liver-modulation of radiation effects by lifestyle-related factors. *Int J Mol Sci* 2018;19:3855.
121. Vares G, Wang B, Ishii-Ohba H *et al.* Diet-induced obesity modulates epigenetic responses to ionizing radiation in mice. *PLoS One* 2014;9:e106277.
122. Nakamura S, Tanaka IB III, Tanaka S *et al.* Adiposity in female B6C3F1 mice continuously irradiated with low-dose-rate gamma-rays. *Radiat Res* 2010;173:333–41.

123. Yoshimoto S, Loo TM, Atarashi K *et al.* Obesity-induced gut microbial metabolite promotes liver cancer through senescence secretome. *Nature* 2013;499:97–101.
124. Dart A. Gut microbiota bile acid metabolism controls cancer immunosurveillance. *Nat Rev Microbiol* 2018;16:453.
125. Haussinger D, Kordes C. Space of disse: a stem cell niche in the liver. *Biol Chem* 2020;401:81–95.
126. Font-Burgada J, Shalapour S, Ramaswamy S *et al.* Hybrid periportal hepatocytes regenerate the injured liver without giving rise to cancer. *Cell* 2015;162:766–79.
127. Wang B, Zhao L, Fish M *et al.* Self-renewing diploid Axin2(+) cells fuel homeostatic renewal of the liver. *Nature* 2015;524:180–5.
128. Tsuchiya A, Lu WY. Liver stem cells: plasticity of the liver epithelium. *World J Gastroenterol* 2019;25:1037–49.
129. Medvedeva NG, Panyutin IV, Panyutin IG *et al.* Phosphorylation of histone H2AX in radiation-induced micronuclei. *Radiat Res* 2007;168:493–8.
130. Dou Z, Ghosh K, Vizioli MG *et al.* Cytoplasmic chromatin triggers inflammation in senescence and cancer. *Nature* 2017;550:402–6.
131. Glück S, Guey B, Gulen MF *et al.* Innate immune sensing of cytosolic chromatin fragments through cGAS promotes senescence. *Nat Cell Biol* 2017;19:1061–70.
132. Turner HC, Shuryak I, Taveras M *et al.* Effect of dose rate on residual γ-H2AX levels and frequency of micronuclei in X-irradiated mouse lymphocytes. *Radiat Res* 2015;183:315–24.
133. Munoz-Espin D, Serrano M. Cellular senescence: from physiology to pathology. *Nat Rev Mol Cell Biol* 2014;15:482–96.
134. Samstein RM, Riaz N. The DNA damage response in immunotherapy and radiation. *Adv Radiat Oncol* 2018;3:527–33.
135. Prise KM, O'Sullivan JM. Radiation-induced bystander signalling in cancer therapy. *Nat Rev Cancer* 2009;9:351–60.
136. Fishbein A, Hammock BD, Serhan CN *et al.* Carcinogenesis: failure of resolution of inflammation? *Pharmacol Ther* 2021;218:107670.
137. Kusunoki Y, Yamaoka M, Kubo Y *et al.* T-cell immunosenescence and inflammatory response in atomic bomb survivors. *Radiat Res* 2010;174:870–6.
138. Barcellos-Hoff MH, Park C, Wright EG. Radiation and the microenvironment - tumorigenesis and therapy. *Nat Rev Cancer* 2005;5:867–75.